General Disclaimer

One or more of the Following Statements may affect this Document

- This document has been reproduced from the best copy furnished by the organizational source. It is being released in the interest of making available as much information as possible.

- This document may contain data, which exceeds the sheet parameters. It was furnished in this condition by the organizational source and is the best copy available.

- This document may contain tone-on-tone or color graphs, charts and/or pictures, which have been reproduced in black and white.

- This document is paginated as submitted by the original source.

- Portions of this document are not fully legible due to the historical nature of some of the material. However, it is the best reproduction available from the original submission.

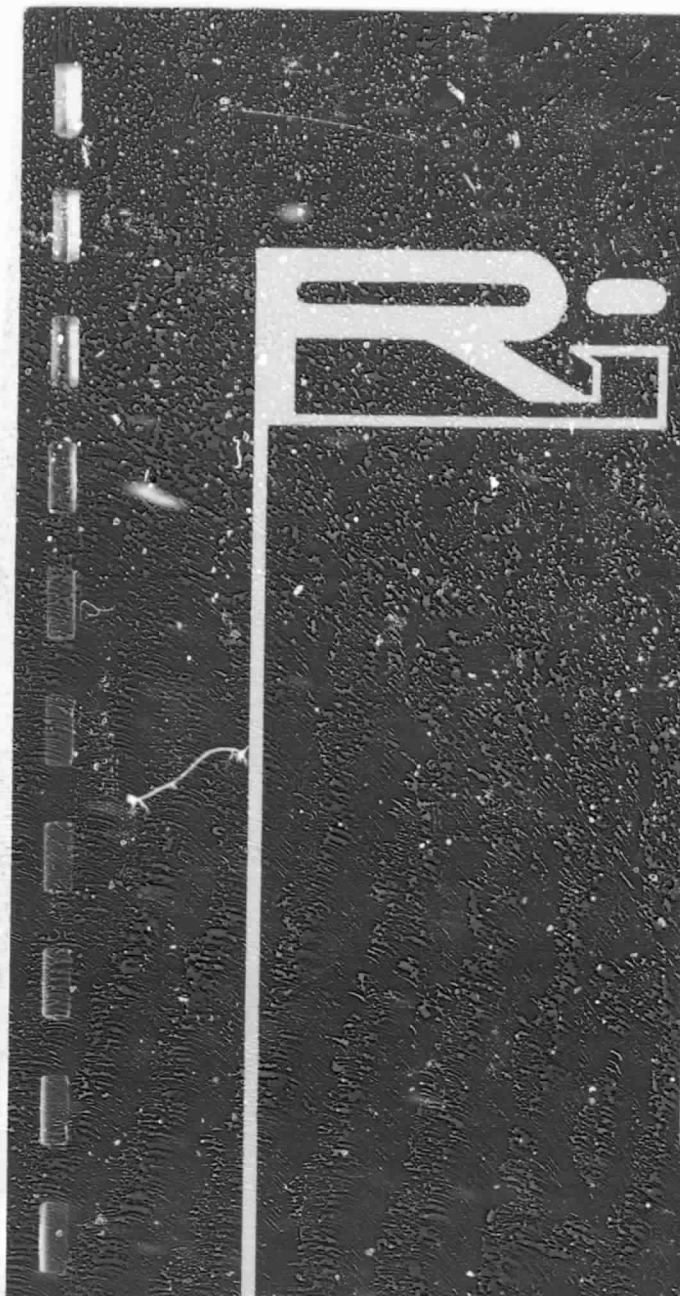

REMTECH inc.

Birmingham, Alabama

REMTECH Inc.
P. O. Box 9083
Birmingham, Alabama 35213

A STUDY draft

ON TURBULENCE MEASUREMENTS

USING LASER DOPPLER SYSTEM

Interim Report On
Contract No. NAS8-25896

27 May 1971

Prepared For

George C. Marshall Space Flight Center
National Aeronautics and Space Administration
Huntsville, Alabama

Prepared by: C. E. Fuller
C. E. FULLER

TABLE OF CONTENTS

Section		Page
1.0	Introduction	1
2.0	Pipe Turbulence Test	2
	2.1 Test Equipment	3
	2.2 Test Procedure	8
	2.2.1 Set up test equipment and conduct pressure measurements	8
	2.2.2 Conduct hot wire measurements	9
	2.2.3 Conduct LDV measurements	10
	2.3 Data Reduction	16
	2.3.1 Static pressure data	16
	2.3.2 Hot wire data	17
	2.3.3 LDV data	18
3.0	Wing Tip Vortex Test	23
	3.1 Wing Tip Vortices	23
	3.2 Test Equipment and Experimental Arrangement	27
	3.3 Vortex Measurements	31
	3.3.1 Doppler spectral distributions	34
	3.3.2 Velocity profiles	36
	APPENDIX	41
	REFERENCES	46
	FIGURES begin on	48

1.0 INTRODUCTION

This interim report documents the work that has been performed by REMTECH Inc. for NASA/MSFC under contract NAS8-25896, titled "Study on Turbulence Measurements Using Laser Doppler System". This work, which was conducted from June, 1970 to June, 1971, has been directed toward the application of a laser Doppler velocimeter system for the three dimensional measurement of gas velocities. Two test programs have been formulated for the application of the system, these being a pipe turbulence test and a wing tip vortex test. The object of the tests was to demonstrate the extent with which the LDV system can be used for the measurement of gas velocities with high spatial and temporal resolution.

At the present time the pipe turbulence test has not yet been started while the wing tip vortex measurements are 90% complete. The pipe turbulence test has been delayed by unexpected time requirements for the modification and preparation of the test facility. A test plan for this test has been completed and is included in this report.

The wing tip vortex test has been underway for several months. This test was planned to provide three dimensional mean velocity data of the vortex pattern shed from a wing tip at an angle of attack. These measurements are being conducted at the MSFC 7 x 7 inch wind tunnel facility and have been quite successful. The test plan and procedure as well as the measurements that have been made are included in this report.

In addition to presenting the test plans for the programs being pursued, data on several measurements of the system's operating parameters which are important to these tests are also included. The status of the programs is also given.

2.0 PIPE TURBULENCE TEST

This section outlines a test for the measurement of turbulent pipe flow using a Laser Doppler Velocimeter system. The purpose of the program is to provide experimental verification of the capabilities of the LDV system for the three dimensional measurement of gas turbulence. A turbulent pipe flow experiment was selected for this purpose because it is both well documented and relatively easy to establish.

The test is to be conducted in MSFC Building 4311 upon completion of necessary modifications. This is expected to be in June 1971. Measurements at the exit of a 4 inch ID pipe will be made with the LDV system. These measurements will include all the values necessary to obtain profiles of the mean and fluctuating velocity components in a plane near the pipe exit. Data reduction is expected to yield frequency spectra for several of the points. The velocity profiles will include 10 to 15 points at a flow Reynolds number, based on the mean flow velocity and pipe diameter, of 250,000. It will be necessary to conduct the majority of the measurements at the pipe exit, since measurements inside the pipe would present several optical alignment problems. Attempts at conducting measurements close to the pipe wall using a specially designed pipe section are also planned. The test parameters and operating conditions are discussed more completely in the subsequent sections.

The sections of this plan include test equipment, test procedure and data reduction. In the first section the operating ranges and characteristics of the test equipment are presented. The section discussing test procedures gives the mechanical and electronic settings which are required to achieve the planned test conditions. The planned test measurements are also presented. These measurements include pressure, hot wire, and laser Doppler. Finally the techniques for reduction of the LDV test data are presented.

2.1 TEST EQUIPMENT

The test equipment which will be associated with this test includes an aerosol generator, pipe flow sections, and the LDV system. This section will duscuss the different test equipment components with emphasis on the characteristics which are pertinent to the planned test.

The aerosol generator is an existing piece of equipment which was designed to provide small submicron tracer particles for previous LDV experiments. The generator produces small liquid particles of Silicon oil by passing high speed air through small jets immersed in the liquid. The maximum design flow rate is 720 SCFM which is above the planned flow rate for this test. Measurements of the particle concentration produced, show concentrations as high as 10^8 particles $/cm^3$ with mean number particle sizes in the submicron range. These values make the generator well suited for this test, since the submicron particles will follow the flow fluctuations well, and the particle concentration is sufficient to provide a continuous Doppler signal at the point being observed.

Figures 1 and 2 show how the generator is to be incorporated into the planned test configuration. The generator, along with the connecting flow sections and pipe length, make up the wind tunnel. The air supply to operate the tunnel is obtained from a 3000 psi source. Two dome loaded regulators will be used to reduce the source pressure to the required operating level. The first regulator will be set at approximately 500 psi and the second regulator will be used to control the actual flow. The air to the aerosol generator will be maintained at 70°F with the use of heaters, in order to maintain constant flow conditions. Several pop safety valves will be incorporated in the system to guard the system against over pressurization which might result from regulator malfunction or operator error.

The generator consists of two levels each containing eight shearing jet nozzles and one by-pass line. The amount of required flow and particle concen-

tration determines how many of the nozzles are to be opened and how much by-pass air is required. Figure 3 defines the expected particle concentration for different ratios of nozzle pressure to tank pressure. The expected generator flow rate for different nozzle pressures and tank pressures is given in Figure 4. In selecting an operating condition for a required flow, it is important to maintain a relatively low flow velocity from the generator liquid bed in order to keep large particles from becoming entrained in the flow and being carried into the flow field. Bed velocities of less than 1 ft/sec have been found to be satisfactory. For this aerosol generator operating at atmospheric pressure, the flow rate through the liquid bed in each level should be kept below 190 SCFM.

As shown in Figure 1, the generator outlet is connected to a flow straightening section, then to a reducing section and then to two sections of 4 inch ID pipe. The flow straightening section contains an 8 inch length of aluminum honeycomb material to break up any large eddies which might be produced at the aerosol generator exit. The reducing section contains adjustable screens which allow for further flow field adjustment to assure a uniform flow into the pipe. A 12 inch strip of coarse sandpaper will be glued to the inside wall at the entrance to the pipe section. This is expected to induce the required turbulent flow within the pipe. In the first pipe section the turbulent velocity profile is expected to be established. The remaining section is the test section. The upstream section has an average wall roughness of 80-100 μ inches RMS and the test section roughness is 20-40 μ inches. Several static pressure tapes, 1/16" diameter, will be located at intervals along the last two sections of pipe. These tapes will provide pressure data from which the pipe frictional coefficient can be calculated.

A modification of the pipe exit is shown in Figure 1 and is designed to allow for measurements into the pipe wall boundary layer. This modification is to consist of a small length of pipe which can be fitted to the pipe exit. This

pipe length will be cut-away on one side to allow for the gathering of scattered light and will have a small hole on the opposite side through which the main laser beam can pass. The hole will be fitted with a glass plug. Measurements of the pipe flow will be made along the laser beam axis up to the hole in the pipe wall. These measurements will not be attempted until the measurements at the pipe exit are completed.

The mean and fluctuating velocity components will be measured in planes located 0.50 and 1.25 inches from the pipe exit. These measurements will be made with the LDV system which consists of a stand, a laser, an LDV instrument and the electronics necessary to process the Doppler frequencies. The stand contains metal supports and adjustment blocks which allow for support and independent adjustment of the laser and LDV instrument. The stand is designed so that the laser is placed on one side of a flow field and the LDV instrument is placed on the other. The laser beam is normally directed through the flow field at right angles to the centerline of the flow facility and then into the center of the LDV instrument. Three scatter tubes and one center tube (referred to as the local oscillator or LO tube) make up the LDV instrument. These tubes contain the optics which collect the LO and scatter beams and direct them onto a photomultiplier tube which detects the Doppler frequency resulting from the homodyning of the two beams. The arrangement of the instrument is such that the three scatter tubes are located at 120° intervals around the LO tube and at an angle, α, with the centerline of the LO tube. Adjustment blocks are available to increase the scatter angle, α, from its normal 8.5° to either 12° , 18° , or 28°. A sketch of the geometrical instrument arrangement and the flow field coordinate system is shown in Figure 5. With the instrument in the normal alignment configuration, i.e. the LO beam at right angles to the flow field centerline, the instrument sensitivity to the W velocity is low in comparison to the sensitivities for the U and V components. This is

especially true for the shallow scatter angle of 8.5°. Increasing the scatter angles on each of the three tubes increases the instrument sensitivity to the W velocity component. The best sensitivity to the W component is achieved with the scatter angle at 28°.

Although increasing the instrument scatter angle will improve the instrument sensitivity, such an increase will increase the path length mismatch between the LO and scatter light paths and also decrease the observed scatter intensity. Both of these effects will degrade the Doppler signal strength which must be maintained in order for the electronic equipment to operate properly. Measurements have shown that the loss in scatter intensity does not cause a significant signal loss. For this reason several additional path length equalizers have been constructed for use during the planned test program. These equalizers will be used to supplement the existing equalizers.

The laser to be used during this program is a Coherent Radiation Laboratory, Model 53, CW argon gas laser. This laser will be operated with an output power of approximately 1.6 watts at 5145 Å. Operation at this power level will not excite any transverse laser modes. When these modes are excited, the homodyning between them results in signal frequencies on the photomultiplier output spectrum which cause difficulty with the electronic frequency trackers.

The electronics associated with the LDV system consists of photomultiplier tubes and power supply, wide band low noise amplifiers, frequency trackers, spectrum analyzers, bandpass filters, RMS and digital voltmeters, and a system for recording the data for further analysis. The electronic network is shown in Figure 6. Perhaps the most important component of the network is the frequency tracker. This instrument is designed to accept the Doppler frequency as input data and to electronically "lock" onto the signal and track the frequency changes. The tracker outputs are a DC voltage corresponding to the mean Doppler

frequency or flow velocity and a fluctuating voltage level (AC) corresponding to the Doppler FM fluctuations or flow turbulence. With the use of the AC and DC calibration curves, the Doppler input frequencies can be identified and used in the equations which relate the geometrical LDV instrument and LO beam arrangement to the Doppler frequency and flow velocity, to obtain the three components of mean and fluctuating velocities.

The trackers are designed to operate over a carrier frequency (corresponds to mean velocity) from 5 to 50 MHz and from 50 to 200 MHz. The frequency deviation can be 0-50% of the carrier frequency (up to 30 MHz) in the wide mode or 0-15% (up to 10 MHz) in the narrow mode. The signal frequency, which corresponds to the turbulence frequency, can be from 0-100 KHz. For this program the trackers are expected to be operated in the 5-50 MHz carrier frequency range, and in the wide mode. In this range the instrument sensitivity is higher and the required input S/N level for proper tracking is 15 dB.

Low pass filters with cut off at 50 MHz are expected to be incorporated at the input to the frequency trackers. These filters will pass only the lower spectrum range in which the Doppler frequency occurs and will block the longitudinal mode frequencies which occur at 95 and 180 MHz. Several bandpass filters will also be used at the AC output of the trackers. These will be set to pass frequencies from 10 Hz to 40 KHz which is the turbulent frequency range of interest.

The data recording system will consist of a wide band tape deck, a multiplexing unit and amplifiers necessary to scale the input data to levels required for recording. The three AC output signals from the frequency trackers will be multiplexed, amplified, and recorded on one channel of the tape deck. The bandwidth of the multiplex and tape deck units will be 20 KHz. The three DC signals from the trackers representing the mean flow velocity will be recorded directly on three input tape channels. The three IF detector signals will also be record-

ed directly on the tape deck. These signals are used to indicate whether the tracker is tracking properly. A change in the DC level of this signal for a period of time, indicates improper tracking for that period. Two other tape input channels will also be required. One for voice identification of the data and the other for a timing marker.

In the next subsection, the operating test procedure for the different equipment components will be presented and discussed in detail.

2.2 TEST PROCEDURE

This section outlines the procedure to be followed in making the flow field measurements. It includes the equipment operating conditions and the measurements that are to be made.

2.2.1 Set Up Test Equipment and Conduct Pressure Measurements

Beginning in June the test equipment will be set up. This equipment will include the aerosol generator and pipe sections which make up the wind tunnel. The aerosol generator and pipe sections are to be arranged as shown in Figures 1 and 2.

First the generator will be placed in position and all the silicon oil drained and cleaned from inside. This is to keep any oil from contaminating the initial pressure or hot wire measurements. Next, the pipe sections will be installed being careful to align and level each section.

Once the tunnel is installed, the following measurements will be made:

1. Determine the pressure setting which will provide a pipe centerline velocity of 143 ft/sec.

   This flow is expected to be achieved from the aerosol generator by opening 5 shearing nozzles in each level with the nozzle pressure at 51.5 psig. The by-pass valve in each level will then be opened until the required velocity is achieved. This velocity can be determined by a pitot tube reading at the pipe centerline and at the pipe exit. The pitot tube should read 4.612 inches of water at

atmospheric static pressure. When the required velocity is reached, the pressures of the regulator panel and the aerosol generator should be noted, since these conditions will be the operating conditions for the test.

2. Determine velocity profiles.

Pitot tube mean velocity profiles will be made at 0.50 and 1.25 inches from the pipe exit. If these profiles are not symmetric about the pipe centerline, adjustments to the screens in the pipe reducing section will be made until the profiles are symmetric. The profiles will be made in both the vertical and horizontal planes passing through the pipe centerline and at radial positions less than v/Ro of 0.90 in order to avoid measurements affected by the shear layer.

3. Static pressure measurements

Static pressure measurements will be made at the ports along the pipe wall using either an inclined manometer or micromanometer. The pressure drop along the pipe is expected to be 0.133 inches H_2O/ft of pipe. Measurements will be made at different intervals along the two pipe sections.

2.2.2 Conduct Hot Wire Measurements

In order to provide data, other than that found in the literature, with which direct comparisons to the LDV data can be made, conventional hot wire data will be taken. Efforts will be made to assure that the positions and profiles of both the hot wire and LDV data are the same.

Single wire data of the U and u' velocity components will be taken at 15 points in planes 0.50 and 1.25 inches from the pipe exit. The points will be in a radial line in the Y and Z directions shown in Figure 7. Values of the turbulent intensity in the X direction will be calculated and used to determine whether the turbulent pipe flow corresponds to the data in the literature. If it doesn't, further adjustments to the screens and roughness elements may be necessary to achieve the desired flow.

Recordings of the hot wire data for spectral analysis will be made at radial distances shown in Figure 8. This data along with the mean velocity and turbu-

lent intensity profiles will be compared to the measured LDV data and the literature data of References 1 through 3. Recordings will also be made of the RMS noise level output in order that the turbulence data can be adjusted for it.

A DISA constant temperature anenometer will be used to make the measurements. The hot wire dimensions of the probe will be 0.66 mm in length and 0.005 mm in diameter. An adjustable sliding block will be employed to position the hot wire during the measurements. A sketch of the test arrangement and electronic connections is shown in Figure 7. Note that the electronic bandpass filter on the RMS voltage output will be set at a low cut-off of 10Hz and a high cut-off of 40 KHz. These are the same filter settings that will be used in the LDV electronic data network.

Techniques for reducing the hot wire data will be given in the section dealing with data reduction.

2.2.3 Conduct LDV measurements

The LDV measurement program is divided into two phases. The first phase is concerned with the instrumentation set-up and calibration. During the second phase, the flow measurements will be made. These two phases are expected to require 7 weeks with some of that time being consumed in data reduction and analysis.

Upon completion of the hot wire measurements, the aerosol generator will be filled with silicon oil and the generator will be turned on to check for proper flow conditions in the pipe. This should be done as before, using the pitot tube at the centerline of the pipe exit. The generator should be operated with five nozzles in each level open and operating at a nozzle pressure of 51.5 psig. The by-pass valves in each level will then be adjusted until the required flow conditions are achieved.

Once the proper flow conditions are established, a measurement of the particle output at the pipe exit will be made in order to obtain values of the output particle size and concentration. Preliminary measurements on the particle generator indicated that the output at the generator outlet at the required operating conditions for this test, will produce a concentration of 1.93×10^8 particle/cm^3 with a mean particle size of 0.8 micron on a mass basis and 0.2 micron on a number basis. Measurements at the pipe exit can be expected to yield lower values of concentration and a possibly larger mean particle size resulting from the wall and screen losses in the pipe and from agglomeration. It is anticipated that the particle output will be satisfactory for the LDV tests; however, periodic particle measurements will be made to be certain. Concentrations lower than 10^6 particles/cm^3 or a mean particle size based on number, larger than 1.0 micron are considered as unacceptable values for this test.

After check-out of the gas flow system, alignment of the LDV instrument will begin. The instrument will be aligned with the LDV instrument at a scattering angle of 28°. At this scattering angle the LDV instrument has the best sensitivity for the three velocity components. This is illustrated by the following list of system sensitivities calculated for the different scatter angles available.

Scatter Angle (degrees)	System Sensitivity mv/ft/sec		
	U Component	V Component	W Component
8.5	8.16	8.16	0.85
12.0	11.78	11.78	1.74
18.0	18.09	18.09	4.04
28.0	27.28	27.28	9.69

During the alignment procedure efforts will be made to minimize the scatter-

ing volume from which the Doppler signal is obtained. These efforts will include the following:

1. Setting the distance between the LO focusing lens and the focal point at 86.0 cm and the distance between the focal point and the end of the LO tube at 56.8 cm. These distances will assure that the LDV instrument will collect scatter light from the smallest focal diameter of the LO lens.

2. The field stop in each of the scatter tubes will be set at 25 microns and the front aperture adjusted for a 15 mm diameter opening. These aperture settings are expected to provide a scattering volume approximately 1.0 mm in length and 0.03 mm in diameter. With a scatter volume of this size and a particle concentration of 10^7 particles/cm^3, the scatter volume should contain approximately 10 particles at all times.

3. Measurements of the scatter volume of all three scatter tubes will be made at the 28° scatter angle. This will be accomplished by moving a small rotating disk with one diffuse surface for scattering through the scatter volume and recording the Doppler signal change as a function of the disk movement. Calculations of the expected scatter volume size are 0.03 for the diameter and 0.22 mm for the length.

The LDV instrument is to be aligned with the pipe exit as shown in Figure 5. The plane in which tube 3 lies will be along the pipe center and the planes of tubes 1 and 2 will each be 30° from a plane parallel to the pipe exit and 90° from the tube centerline. With the instrument in this configuration, the signal from tube 3 will be composed of velocity data in both the X and Z directions. The output from this tube will be checked against the anticipated output shown in Table 3 of the Appendix. The techniques for calculating these values are outlined in the Appendix. The tube 3 output will offer an on-the-spot check of expected system operation thus decreasing the chances of recording and reducing data which may be incorrect.

Before beginning the LDV measurements, the electronic components will be checked for proper operation. Each of the frequency tracking units will be calibrated using known input signals. These calibrations are expected to agree with

the factory calibrations shown in Figures 9 and 10. The calibration procedure will consist of tracking input signals, along with the PM tube noise, over a frequency range from 5 to 50 MHz and at frequency deviations of 0-50% of the carrier frequency. The DC voltage corresponding to the different input frequencies will be recorded. The RMS voltage at the AC output will likewise be recorded. When the carrier frequency is undeviated, the RMS values will correspond to the system noise level. This noise level is expected to be 4mv RMS with the bandpass filter at a low cut-off of 10Hz and a high cut-off at 40 KHz.

The multiplexing and data recording system will also be checked for accurate operation over the dynamic input range expected for the planned tests. These input ranges are given below:

1. Three AC inputs with a frequency range from 10 Hz to 40 KHz and a voltage level from 4 to 100 mv RMS.

2. Three AC signals from the IF detector. This signal is normally at a DC voltage level of 11 volts when the tracker is tracking properly. When the tracker has a temporary loss in signal, the voltage level drops to 0 with a fall time of less than 100 μs and recovers lock at a rise time of 0.1 to 1.0 millisec.

3. Three DC signals with voltage levels from 1.0 to 5.0 volts.

4. One input will also be used for voice identification of data and one input will be used as a time marker.

Once the LDV instrument is aligned and the electronic equipment is checked, actual data measurements will begin. The position of points to be taken are given in Figure 11. Note that before the LDV data is recorded for data reduction, preliminary checks of the system accuracy can be made by comparison with the anticipated values for tube 3 given in Table 3 of the Appendix. All AC and DC voltages will be read and recorded on paper at the same time the data is being tape recorded. These values will be used for comparison with values computed for the tape recordings.

It will be necessary to provide calibration signals on each of the data input

channels for the tape recorder. The procedure for tape calibration is as follows:

1. Set the appropriate data amplifier or attenuator so that the anticipated data input signal does not exceed the tape limits of 1.0 volts RMS.

2. Input at least 5 seconds of calibration signal into each of the data input channels except the IF detector inputs.

3. Identify each of the calibration inputs on the voice channel. These inputs should be identified by the value input to the amplifiers or attenuator rather than the value input on the tape.

Each data point should be recorded for at least 5 sec. The voice channel will be used to identify the X, Y, Z position of the data. It will be of utmost importance to maintain the Doppler signal to noise level as high as possible. With the tracker operating in the wide mode, the minimum S/N specified by the manufacturer for proper tracking is 15dB. It is felt that an S/N level of 20 dB be maintained during the measurements in order to be confident of the tracker operation. If an S/N level of 20 dB cannot be achieved or maintained, the following items should be checked as possible causes.

Insufficient scatter intensity - This condition exists when the PM anode voltage reading is less than 100 mv for the scatter light with the PM tube at an operating voltage of 800 volts.

1. Low incident laser power - Laser power from the CRL Model 53 should be at least 1.6 watts at 5145 A. Note that laser power should not be adjusted to cause mode beat frequencies to occur on the PM tube output spectrum, since such frequencies can result in unstable tracker operation.

2. Low particle concentration - The desired concentration level is 10^6 particles/cm^3 with mean particles less than 1.0 micron. Check the level and temperature of the oil in the aerosol generator. Adjustments in the by-pass or nozzle controls valves may also be necessary.

3. Apertures closed - Front aperture should be at 15 mm diameter and field stop at 25 microns.

4. Misalignment of the scatter tube - Check for proper alignment by either movement of the front refractor plate until maximum PM

anode voltage is obtained or by movement of the entire scatter tube with the cross block adjustments. Note that cross block adjustment will necessitate the re-alignment of the other tubes.

5. Improper focusing at the scattering volume - the scatter volume should occur at the intersection of the focused LO beam and the focal point defined by the optics in the scatter tube. The focal distance for the LO focusing lens is 86.0 cm. The scatter tube should be adjusted to receive maximum scattered light when a scattering source such as a small alignment jet is placed at the LO focus.

Improper path length equalization - Adjust the path length equalizers until the S/N is maximum.

Misalignment between the scatter and LO beams

1. Angular misalignment - Adjustments to the LO refractor plate and the beam splitter in the scatter tube are used to achieve angular alignment.

2. Beam size misalignment - The size of the LO beam may be increased or decreased with the use of the aperture stop in the LO tube.

Low LO intensity - Adjust the LO attenuator until the intensity is at least five times greater than the scatter intensity.

Improper PM tube voltage and/or amplifier settings - the PM tube voltage should be set at 800 volts and the amplifier voltage at 14 millivolts.

Bad PM tube - Replace

After recording a set of LDV data, it will be processed by computer techniques. These techniques are described in the following section.

2.3 DATA REDUCTION

In this section the techniques for data reduction will be discussed. It is anticipated that the hot wire data will be reduced by hand computations except for computer computations and plottings of the frequency spectrum of several points. The LDV data will be reduced entirely by computer techniques.

2.3.1 Static Pressure Data

The measurement of the static pressure loss or head loss down a pipe in incompressible flow can be shown to be related to the friction factor or pipe friction coefficient by the following expression

$$f = \frac{2\Delta P\ D}{\rho\ V^2 L} \qquad (1)$$

where
- f = friction coefficient
- ΔP = pressure change over the length L - lbf/ft^2
- V = the average, over a cross section, of the mean-time average velocity. This is equivalent to the volume flow rate divided by the cross sectional area.
- D = pipe diameter - ft
- L = length of pipe over which the pressure change is to be determined - ft.
- ρ = gas density - $lbf\ s^2/ft^4$

Expression (1) may then be used to calculate the friction coefficients for pipe to be used in this test. The expected value of f is 0.015 corresponding to a Reynolds Number of 250,000 and a smooth pipe. Care must be taken in the control of the pipe velocity since slight changes will result in corresponding changes in the friction coefficient. The expected pipe pressure loss is 0.133 inches H_2O/ft of pipe. Thus in order to maintain a measurement accuracy of 1% the pressure should be read to within a thousandth inch of H_2O.

Now if a force balance is considered for a cylinder whose periphery touches the pipe, the following relation can be obtained for the wall shear stress.

$$\tau w = \frac{f\ \rho v^2}{8}$$

Using the measured velocity profiles the relation between V, mean average velocity, and V_{CL}, centerline velocity can be determined and the following value defined.

$$\frac{\tau w}{\rho V_{CL}^2} = K$$

This value of K will define the intercept of the Reynolds shear stresses $\overline{u'v'}/V_{CL}^2$ with the pipe wall. It can be shown that the radial variation of total shear (turbulent + viscous shears) is linear with radius. With the exception of a very thin region near the wall, the viscous shear is a minor portion of the total shear and thus the turbulent shear stress $\overline{u'v'}$ has essentially a linear distribution. Measurement of the Reynolds shear stress term, $\overline{u'v'}/V_{CL}^2$ with the LDV system would be expected to fall along the defined linear region.

2.3.2 Hot Wire Data

The hot wire data will consist of a radial profile at x = 1.25 inches. The points to be taken in this profile are given in Figure 8.

The hot wire data reduction will conform to the standard techniques for data reduction as outlined below.

Mean Velocity

In order to make mean velocity measurements, it is necessary to calibrate the probe with a pitot probe. With both the pitot probe and hot wire mounted along side each other in a constant uniform velocity region, the values read by each should be plotted as DC voltage versus velocity for the velocity range of interest. In this case, the velocity range will be from 150 to 75 ft/sec. corresponding to a pitot tube pressure of 5.017 and 1.254 inches of water.

The DC voltages at the desired points can then be read and a corresponding mean flow velocity determined.

Fluctuating Velocity (Turbulence)

The voltage related to the turbulence intensity will be read

as a root mean square voltage. This voltage can be written as

$$\overline{V^2 read} = \overline{(V\ signal + V\ noise)^2}$$

where V signal = the instantaneous signal voltage resulting from the flow fluctuations

V noise = the instantaneous electronic noise voltage measured with no signal present.

Then assuming that there is no correlation between the signal and the noise voltage, i.e.

$$\overline{V\ signal\ V\ noise} = 0$$

Then $\overline{V\ signal^2} = \overline{V\ read^2} - \overline{V\ noise^2}$

Note that the voltage read during the test measurements can then be corrected for the noise level.

Once the RMS signal voltage is obtained, the following expression can be used to obtain the turbulent intensity level;

$$\text{Percentage of turbulence} = 100 \cdot \frac{\overline{V^2\ signal}}{} \cdot 4V/V^2 - V_o$$

where V_o = DC voltage at zero flow velocity

V = DC voltage at the measured position

- Turbulence Spectrum Analysis

The turbulent voltage data which is to be recorded on tape will be reduced by computer analysis. The computer will compute the correlation function given as

$$R_e(\tau) = \frac{\overline{V(t)\ V(t+\tau)}}{\overline{V\ (t)^2}}$$

from which the energy spectrum may be found as

$$F(n) = 4\int_o^\infty Re\ (\tau) \cos 2\pi n\tau d\tau$$

where n = frequency
τ = time interval
V = velocity

2.3.3 LDV Data

The data reduction techniques for the LDV system are more complicated than the techniques for the hot wire data, due to the necessity of having

three components rather than one. Each of these components are related to each other through the following equations.

$$A_1 e_1 = 1/2\, a_{31} u - a_{12} v - a_{13} w$$

$$A_2 e_2 = 1/2\, a_{31} u + a_{12} v - a_{13} w \qquad (3)$$

$$A_3 e_3 = a_{31} u + a_{13} w$$

where e_i = Tracker voltage output

u, v, w = Velocity components

a_{ij} = Angular orientation coefficients

A_i = Tracker calibration

Also $u = \bar{u} + u'$

$v = \bar{v} + v'$

$w = \bar{w} + w'$

and $e = \bar{e} + e'$

where the barred values represent the mean velocity or voltage and the primed values represent the fluctuating velocity or voltage. Equation (3) can then be rewritten in terms of either mean velocity or fluctuating velocity as

$$A_1 \bar{e}_1 = 1/2\, a_{31} \bar{u} - a_{12} \bar{v} - a_{13} \bar{w}$$

$$A_2 \bar{e}_2 = 1/2\, a_{31} \bar{u} + a_{12} \bar{v} - a_{13} \bar{w} \qquad (4)$$

$$A_3 \bar{e}_3 = a_{31} \bar{u} + a_{13} \bar{w}$$

and $$A_1 e'_1 = 1/2\, a_{31} u' - a_{12} v' - a_{13} w'$$

$$A_2 e'_2 = 1/2\, a_{31} u' - a_{12} v' - a_{13} w' \qquad (5)$$

$$A_3 e'_3 = a_{31} u' + a_{13} w'$$

Of particular importance in this test is the reduction of the turbulence data as given in equation 3. The desired turbulence related values will be $\sqrt{\overline{u'^2}}/\bar{u}_{cL}$, $\sqrt{\overline{v'^2}}/\bar{u}_{cL}$, $\sqrt{\overline{w'^2}}/\bar{u}_{cL}$, $\sqrt{\overline{u'v'}}/\bar{u}_{cL}$, $\sqrt{\overline{u'w'}}/\bar{u}_{cL}$, $\sqrt{\overline{v'w'}}/\bar{u}_{cL}$, and the frequency spectrum of the three velocity components. All of these values can be computed once the velocity components defined by equations 4 and 5 are solved. The solution to the desired turbulence values as defined by equation 5 can be made if the following expressions are known:

$$\overline{e_1(t)'^2},\ \overline{e_2(t)'^2},\ \overline{e_3(t)'^2},$$

$$\overline{e_1(t)'\ e_2(t)'},\ \overline{e_2(t)'\ e_3(t)'},\ \overline{e_3(t)'\ e_1(t)'},$$

$$\overline{e_1(t)'\ e_1(t+\tau)'},\ \overline{e_2(t)'\ e_2(t+\tau)'},\ \overline{e_3(t)'\ e_3(t+\tau)'},$$

$$\overline{e_1(t)'\ e_2(t+\tau)'},\ \overline{e_2(t)'\ e_3(t+\tau)'},\ \overline{e_3(t)'\ e_1(t+\tau)'},$$

$$\overline{e_2(t)'\ e_1(t+\tau)'},\ \overline{e_3(t)'\ e_2(t+\tau)'},\ \overline{e_1(t)'\ e_3(t+\tau)'}\ ,$$

It is anticipated that these values will be computed by existing computer programs at MSFC. The use of these values can be illustrated by the following.

In the computation of the spectral distribution the correlation function defined by

$$R_e(\tau) = \frac{\overline{u'(t)\ u'(t+\tau)}}{\overline{u'(t)^2}} \qquad (6)$$

must be computed.

The instantaneous value of u' as defined by equations 5 is

$$u' = 1/3a_{31}\ (A_1 e_1' + A_2 e_2' + 2\ A_3 e_3') \qquad (7)$$

substituting in equation 6 yields for the numerator

$$1/9a^2_{31}\Big[A_1^2\,(\overline{e_1'(t)e_2'(t+\tau)}) + A_2^2\,(\overline{e_2'(t)e_2'(t+\tau)}) + 4A_3^2(\overline{e_3'(t)e_3'(t+\tau)}) + A_1A_2(\overline{e_1'(t)e_2'(t+\tau)} + \overline{e_2'(t)\,e_1'(t+\tau)}) + 2A_1A_3(\overline{e_1'(t)\,e_3'(t+\tau)} + \overline{e_3'(t)\,e_1'(t+\tau)}) + 2A_2A_3(\overline{e_2'(t)\,e_3'(t+\tau)} + \overline{e_3'(t)\,e_2'(t+\tau)})\Big] \quad (8)$$

Similar expressions can be written for the various other computations required. These computations do not consider any electronic noise.

Since an electronic noise level is known to exist at the tracker output, the recorded tracker data will consist of both signal and noise. The tracker output can be written as

$$e_o' = e_1' + e_{n1}' \quad (9)$$

where

e_1' = instantaneous voltage due to Doppler signal

e_{n1}' = instantaneous voltage due to the noise

e_o' = instantaneous voltage output

If expression 9 is solved for the signal voltage and substituted in equations 3, a different set of computations will be required, in order to allow for the noise. These computations require that the noise terms be time averaged with themselves and the signal terms. A number of simplifications can be made within the noise expressions if the noise is "white" or purly random. In this case, most of the time averaged terms involving the noise will be zero and only those terms involving the time average of the noise squared from each

tracker will remain. Such a simplification would be helpful in the data reduction techniques; however, the tracker noise has not been found to be random. Measurements have shown that the tracker noise consists of strong 60 and 120 CPS frequencies which can be expected to correlate with themselves and the other cross terms. For this reason the data reduction will be more complicated.

The turbulent LDV quantities will be compared with the measured hot wire data and the data of References 1 through 3. These comparisons will be used to establish the capabilities of the LDV system for three dimensional turbulence measurements.

3.0 WING TIP VORTEX TEST

In the past year, interest in the phenomena known as wing tip vortices has increased considerably. This has been largely brought about by the advent of large military and commercial aircraft which produce strong vortex patterns which persist for some time and represent a dangerous flight region for smaller aircraft. For this reason, many efforts both theoretical and experimental are being undertaken to expand the knowledge of wing tip vortex flows so their behavior can be accurately predicted. Since the vortex flow is highly three dimensional, the use of the MSFC LDV system to study vortex patterns was apparent since it offered a capability for three dimensional measurement without the use of a physical probe within the flow field.

The following sections give some theoretical and experimental considerations found in the literature and describe the measurements that have been made to date with the LDV system.

3.1 WING TIP VORTICES

When fluid flows past a lifting wing trailing vorticity is produced which, at some distance behind the wing, eventually concentrates into two trailing vortices of opposite circulation. These vortices results from the upwash around the wing tip and the eventual rolling up of the vortex sheet shed from the wing trailing edge.

Previous investigators have provided different approaches to the explanations of the vortex flow structure. The approaches using inviscid or laminar concepts have been found to disagree with wind tunnel and field measurements. It is,therefore, most likely that the vortex flow must be approached with turbulent considerations.

Hoffman and Joubert (Reference 4) attempt to establish the laws governing

the flow in a turbulent line vortex. They use an approach similar to the methods used in turbulent boundary layer theory, to predict that the circulation in a region of the vortex is proportional to the logarithm of radius under certain conditions. Inside this region, the fluid should rotate as a rigid body (tangential velocity α radius) and outside of it the circulation should approach a constant value. Neglecting any radial velocity variations, they find that for a fully turbulent vortex a "universal" circulation curve exists when the parameter, $Uz/\Gamma_o > 150$, where U is the free stream velocity, z is the distance downstream from wing and Γ_o is the free stream circulation. From this circulation curve the distribution in vortex tangential velocity with radius is given in terms of the peak tangential velocity and the radius at which it occurs. Comparisons with experimental data show good agreement with predicted profiles for conditions at which the profiles apply. They conclude by pointing out that although their development shows promise for the data presented, further experiments are needed to extend and verify their results for different vortex generation techniques, and for the growth and development of vortices.

Newman (Reference 5) linearizes the equations of motion for an isolated laminar viscous vortex at moderate to large Reynolds number, by assuming that both the rotational velocity and the deficit of longitudinal velocity are small compared with that in the free stream. He compares his solution with pressure measurements in a turbulent vortex and notes that fair agreement can be obtained by applying an effective eddy viscosity to his laminar solution.

Dosanjh and others present comparisons of Newman's solution with three-dimensional velocity data calculated from directional pressure probe measurements. Their data was taken at distances close to the vortex producing airfoil and at Reynolds number based on the free-stream velocity and chord length of

10,000. Although their investigations were intended to be of a laminar vortex, they note that turbulence levels of 3% were measured during their tests. The comparisons which they present with Newman's solution show good agreement when an effective viscosity 8-10 times the laminar kinematic viscosity was used. The agreement is especially good close to the vortex center and for downstream where flow axi-symmetry are better.

Although Dosanjh's test does not compare identically with the LDV vortex test (primarily a difference of Reynolds number - the LDV test has a Reynolds number 35 times larger) the three dimensional data can serve as a basis of comparison for the LDV data. No other three dimensional velocity data has been found.

Spreiter and Sacks (Reference 7) developed theoretical relations for the motion of trailing vortices associated with a lifting wing in subsonic and supersonic flows. Their analysis is of interest since they derive expressions which define the degree to which a vortex is rolled up in terms of the distance behind the wing, the lift coefficient, span loading and aspect ratio of the wing. From these expressions estimates of the vortex core size (Figure 18) and the degree of vortex formation can be made for the LDV wind tunnel tests.

Another study which is of interest when considering turbulent vortices is that of McCormick, Trayler and Sherieb (Reference 8). They present both field and wind tunnel studies of vortex patterns which indicate that vortices generated immediately behind the wings of small aircraft (Army O-1 and Piper Cherokee) follow the laminar vortex behavior, and then undergo a transition to the logarithmic form at some distance downstream. They hypothesize that this change may be associated with vortex breakdown rather than transition. Their data generally show good comparisons with Hoffman and Jorbert's turbulent vortex analysis.

Although many theoretical and experimental studies have been conducted on vortex flows, it appears that no approach has completely described the phenomena without making several simplifying assumptions for convenience of the analysis and available data. The three dimensional data which will be made available with the LDV system can be expected to present a more precise picture of the flow than prior investigations have furnished. This data will be valuable in the formulation of a more complete theory of vortex flows.

In the following sections the LDV vortex test program is described and the current data presented.

3.2 TEST EQUIPMENT AND EXPERIMENTAL ARRANGEMENT

The LDV vortex tests are being conducted at the MSFC 7"x 7"Inch Wind Tunnel which is an atmospheric to vacuum blow down tunnel. For these tests the tunnel is operated at subsonic flows, the speed being set by locking an adjustable diffuser in place. The tunnel air supply consists of atmospheric air which is dried and stored in a tank provided with a rubber diaphragm to maintain constant supply pressure during blow down.

A test section, 7"x7", is accessible by complete side wall removal, accomplished by hydraulic cylinders. For the vortex test, a 6% - thick biconvex constant cross-section wing with an aspect ratio of 2.7 was attached to the tunnel side wall (door) at a +6° angle of attack. The wing had a chord of 2.59 inches and a semi-span of 3.5 inches. The trailing edge of the wing was at the upstream edge of the sidewall observation window and the wing tip was along the tunnel centerline. A schematic of the tunnel and LDV system arrangement is shown in Figure 12.

The LDV system components used for the vortex measurements are essentially those described in the section dealing with pipe turbulence. However, several differences in the system arrangement might be noted. One difference is that an acousto-optical modulator is used to shift the frequency of the LO beam either by 19.6 or 57.6 MHz depending on the settings. This shifted laser light was necessary to determine the direction of the velocity components.

Another difference is the technique for identifying the Doppler frequency. In the pipe turbulence test the frequency trackers are to be used; however, it has been found that the trackers will not track the Doppler signals when the modulator is used because the modulator operation produces strong frequencies at either 19 or 57 MHz which the tracker will lock onto. For this reason another technique was used for this test. The schematic arrangement of the electronic

equipment used for this technique is shown in Figure 13. In this technique the three Doppler frequencies were initially processed by three spectrum analyzers. An ability to improve the S/N displayed by the spectrum analyzers was provided by a signal analyzer (Hewlett-Packard Model 5480) which processed the vertical output of each of the spectrum analyzers. The spectral display on each spectrum analyzer is stored in the signal analyzer as a series of 250 points in a magnetic core. The Doppler spectral display may then be recorded using an X - Y plotter or the maximum point on the spectral display identified by placing a frequency generator signal at the peak of the Doppler display, as observed on the oscilloscope display of the signal analyzer. The frequency at the maximum point is then countered as the mean Doppler frequency. This countering technique has been used for all the vortex data. The spectral analyzer widths were kept at 1 MHz/cm during the majority of the measurements. This allowed for a greater precision in identification of Doppler frequency since each dot or point on the signal anaylzer display would be 40 KHz. A precise identification of the Doppler frequencies was important in order to maintain an acceptable accuracy level for the velocity components.

The scatter angle and arrangement of the LDV instrument is another difference in the system for vortex measurements from that of the pipe turbulence test. The scatter angle used for these tests was $12°38'$ and the instrument was sitting so that scatter tubes were arranged as shown in Figure 12 with respect to the wind tunnel flow. For this instrument in this arrangement and for this scatter angle the mean Doppler frequency components are given by the following expressions

$$F_1 = 0.66\ C_2\ v + 0.33\ C_3 w$$

$$F_2 = -0.50\ C_1 u - 0.33\ C_2 + 0.33\ C_3 w$$

$$F_3 = 0.50\ C_1 u - 0.33\ C_2 + 0.33\ C_3 w$$

where C_i are functions of the angular arrangements of the instrument relative to the velocity coordinate system, and u, v, and w are the orthorgonal velocity components with directions as shown in Figure 12. For any particular instrument arrangement the values C_1 , C_2 and C_3 are constants.

The sensitivities of the Doppler frequencies to changes in the velocity components can be noted in the following list of partial derivatives.

$$\frac{\partial F_1}{\partial u} = 0 \qquad \frac{\partial F_2}{\partial u} = -0.1122 \qquad \frac{\partial F_3}{\partial u} = 0.1122$$

$$\frac{\partial F_1}{\partial v} = 0.1295 \qquad \frac{\partial F_2}{\partial v} = -0.0647 \qquad \frac{\partial F_3}{\partial v} = -0.0647$$

$$\frac{\partial F_1}{\partial w} = -0.0143 \qquad \frac{\partial F_2}{\partial w} = -0.0143 \qquad \frac{\partial F_3}{\partial w} = -0.0143$$

It is instructive to note that the instrument arrangement for this test is least sensitive to changes in w velocity components and most sensitive to changes in the u and v velocity components, the difference in sensitivities being approximately an order of magnitude. This lack of sensitivity to the w velocity component means from a practical measurement standpoint that the Doppler frequency components must be identified very precisely in order for the w component to be meaningful. For example a frequency error of ± 0.1 MHz in any Doppler frequency component would cause a w velocity error of ± 7.0 ft/sec.

For these tests the optical settings on the instrument were such that the smallest scattering volume is the region from which the Doppler shifted light is received and is equivalent to the probe of conventional measuring techniques. For this test the scattering volume was found to be essentially a cyclindrical region 0.03 mm in diameter and 0.5 mm in length.

For alignment of the LDV instrument a positioning stand containing a needle

jet of 0.018 of an inch inside diameter was constructed. This stand was designed so that it could be clamped in the wind tunnel and the needle tip positioned at precise locations inside the wind tunnel. Once the needle was positioned, a small air flow containing silicon oil particles was passed out the needle, thus forming a small jet of air and particles. The laser beam was then passed across the tip of the needle so that it just grazed the tip. The stand and laser beam were then moved up 0.020 inch and the beam was adjusted so that the beam was centered in the jet flow. With the laser beam thus located in the small jet, the LDV scatter tubes were aligned so that they were receiving scatter light from the jet and ultimately a Doppler signal from each scatter tube was obtained and maximized. This jet furnished the point relative to the wind tunnel from which all the measurements were made.

The particles in the tunnel flow which provided the Doppler frequency shift in the laser light were liquid silicon particles produced by forcing compressed air through a series of shearing jets immersed in a bed of the liquid. Measurements of the particle concentrations and sizes used for this test indicated that particle concentrations of 2.08×10^6 particles/cm^3 with a mean number particle size of 0.30 micron were available in the air supply sphere. While wind tunnel measurements were being made the particles were continuously injected into the supply sphere. A more complete description of the aerosol generator is given in Reference 9 .

3.3 VORTEX MEASUREMENTS

This section describes the types of measurements that have been made, the meaning of the measurements, and the difficulties encountered. At this time, neither these measurements nor their analysis have been completed. The measurements are expected to be complete in late June, however, the analysis of the data may require several weeks longer.

These measurements were intended to demonstrate the ability of the LDV system for vortex type measurements as well as provide data defining the flow in a wing tip vortex pattern. The measurements were initially begun at 7.0 inches (one wing span) from the wing trailing edge and then moved to 14 inches downstream or 2 spans. The data measurements that have been made are tabulated in Figure 15. This tabulation shows the number of data points made at the various tunnel locations. The X, Y and Z values refer to the location of the coordinate system shown in Figure 12. All the measurements have been at a tunnel free stream velocity of 278 ft/sec as measured by a static pressure tap. All the profiles are in the Y direction since this is the direction in which the system is most easily and accurately moved.

Most of the measurements made up to 3/25/71 were used to establish measurement techniques and establish confidence in the data and its accuracy. The data following that date was found to be the most accurate and useful.

Several difficulties have been encountered in this measurement program. These include vibrations in the test area, unstable electronics, wind tunnel movements, and reduced particle concentrations in the core region. The vibrations in the test area were caused by the periodic operation of several large compressors located nearby. These vibrations produced amplitude modulations of the Doppler signals caused by fluctuations in the laser beam intensity and shifting of the scatter and LO beam alignment. Although the vibrations were never severe

enough to cause total instrument misalignment, they were a particular nuisance when measurements were being made close to the vortex core where the signal's strengths were low. Some vibration absorption pads which were placed under the instrument stand had no noticeable effect on reducing the vibration of the instrument. Since the vibrations were not continuous, that is the pumps only operated depending on the pressure required, the usual procedure followed during the LDV tests was to wait until the pumps quit before making measurements.

As explained in Section 3.2 it is necessary to maintain a measurement of at least ± 0.050 MH on each Doppler frequency component in order to maintain an accuracy of ± 10.5 ft/sec in the w velocity component. For this reason all the electronic equipment must be in accurate operating condition. During the period in which data has been taken, two of the spectrum analyzers were found to be unstable. This unstableness although slight caused doubt to be reflected on some of the data that had been taken up to that time, especially on the w velocity component.

Another difficulty was caused by slight movements of the wind tunnel along its axis. Such movements meant that the X position of the scattering volume relative to the wind tunnel was not located at 7.00 or 14.00 inches as expected. This axial movement of the tunnel is caused by the changes in pressure in the vacuum field to which the tunnel is connected. The tunnel movement has most often been noticed when the 14 x 14 inch tunnel, connected to the same vacuum field runs and causes the vacuum pressure to build up. Movements of as much as 0.014 of an inch in the axial direction have been measured. Since the vortex velocity field does not change rapidly in the axial direction, any slight movement of the tunnel would not be expected to be noticed in the measurements and none have been. The tunnel movement problem is most annoying when attempting to check the system alignment using the needle jet. Since the needle jet stand is attached to the

tunnel it moves as the tunnel moves and the jet moves out of the laser beam and the alignment Doppler signals are lost until the tunnel returns to its original position which it usually does.

The fact that the particle concentration in the vortex region is less than in the other tunnel flow presents two problems. One is that the reduced concentration results in a reduced Doppler S/N level. This is especially unfortunate in the vortex core region since, the nature of the flow, i. e. large velocity gradients (at least as high as 800 ft/sec/inch) and possibly high turbulence levels, would cause a broadening of the Doppler signal and a corresponding S/N reduction even if the particle concentration were constant. The reduced particle concentration makes it even more difficult to obtain data in the core region. The cause of the particle reduction may be of even more concern, when considering measurements in the core. The lack of particles in the core is most probably a result of radial forces acting on the particles to sling them away from the core center, to a point where these forces are balanced by the aerodynamic drag forces on the particles. The motion within the core, i.e. V tangential α radius, is such that any particle placed in that region will be forced out of it. Such a phenomena implies that the particle and fluid paths are not approximately equal.

The reduced particle concentration in the core region can be qualitatively observed in the pictures of Figure 16. These pictures were made from frames of a movie film of the vortex flow 8.0 inches from the wing trailing edge. The flow field was illuminated by a thin sheet of laser light passing through the wind tunnel at that position. The pictures were made at a 42° angle with the tunnel center line and looking upstream. The pictures not only show the core region but also the spiral nature of the flow.

This lack of particles in the core region as well as the nature of the flow has caused a loss of Doppler signal in the majority of the attempts to conduct

measurements in that region. To date only one profile in which all Doppler signals have been maintained, has been made close to the core region. That was the profile made on April 22, 1971. The fact that the signals were maintained on that profile indicates that data can be obtained in the core region, however, the difficulty in achieving such measurements is pointed out by the number of prior attempts which have been made.

The following two subsections discuss the data which has been taken.

3.3.1 Doppler Spectral Distributions

Throughout these measurements the Doppler spectral distributions in the vortex region have been of concern primarily because of a necessity of maintaining a good accuracy in the identification of the mean Doppler frequencies. The term mean Doppler frequency is taken to be the frequency at which the Doppler spectrum has a maximum signal intensity. This maximum point on the Doppler spectrum is the point at which the mean frequency has been identified for all the measurements presented.

Figure 17 shows some typical Doppler spectrums for the F_1 frequency component.

As noted in Section 3.2 the F_1 frequency component has no sensitivity to the u velocity component, is most sensitive to the v component and approximately an order of magnitude less sensitive to the w component. The v velocity component will roughly correspond to the vortex tangential velocity for measurements made close to the vortex core. Since the tangential velocity distribution as sketched in Figure 18, exhibits rather high velocity gradients and since the long dimension (0.5 mm) is such that it sees this velocity spread, and further that the F_1 frequency component is most sensitive to this velocity, one would expect to observe a broad signal on F_1 when measurements are made close to the core. The spectrums of Figure 17 do in fact show this to be the case. The signal in the top trace

which is outside the core region is rather narrow and Gaussian in shape. The identification of the mean Doppler frequency at the peak intensity point is quite accurate for that measurement. Now note the changes in the signal trace as the core region is approached. The signal has definitely broadened to the point that a peak on the trace is rather hard to identify. The term mean Doppler frequency is much harder to define since the signal strength is widely spread and not symmetrically distributed. Besides becoming broader the signal intensity is reduced due to the reduced particle concentrations. This signal broadening and intensity reduction is even more evident in the series of F_1 spectrums shown in Figure 19.

Another characteristic of the F_1 Doppler spectrum is noted in the bottom trace of Figure 17. This trace shows a double hump in Doppler signal intensity. This type signal may be caused by a segregation of particles in the vortex region. The larger particles would tend to be located further from the vortex center with the smaller particles located closer to the center. The larger particles would produce a larger scatter of laser light and would therefore, be expected to produce a higher intensity Doppler signal. On the other hand, the smaller particles would produce less scatter and less Doppler signal per particle, however, the number of smaller particles could be expected to be greater than the large ones. It therefore, seems that such a particle segregation might cause the observed Doppler spectrum.

Since the nature of the Doppler spectrum near the core is rather broader and open to some amount of interpretation as to where the mean Doppler signal is located and also the core region is rather small, it was felt that the accuracy of the measurements could best be maintained by making measurements at a very close spacing. This spacing was 0.005 of an inch at points in the core region. Points at such a spacing allowed for a certain signal overlap since the scatter-

ing volume length was approximately 0.020 of an inch. This signal overlap also helped to smooth any fluctuations or difference in the flow field from run to run, since only one point was made per operation of the wind tunnel.

So far in this discussion of Doppler spectral distributions no mention has been made of the effects of turbulence on the observed signal broadening in the core region. An increase in turbulence intensity would definitely broaden the observed spectrum. Several investigators (References 4 & 5) attributed observed wing tip vortex behavior to an increased turbulence level in the core region. Before concluding the vortex investigations it is intended that measurements in the core region will be made with the frequency trackers. By using the output from the frequency trackers the turbulence intensity in the flow can be determined.

3.3.2 Velocity Profiles

In making a velocity profile for this test the following procedure was followed:

1. All electronic equipment was turned on and the laser was started.

2. The small needle jet was placed in the tunnel and the laser beam was adjusted so that it passed through the center of the jet and 0.020 of an inch from the exit. Before directing the laser beam through the jet, the laser power was maximized at 2.5 - 3.0 watts multi-mode at 5145 Å.

3. Then the refractor plate on each scatter tube was adjusted slightly until a Doppler signal was obtained on each spectrum analyzer. Slight adjustments of the beam splitters on each tube was also usually necessary to maximize the signals on each tube (30-35 db-S/N).

4. It was usually necessary to let the laser warm up for approximately 1 hour or until the output power stabilized, before beginning data taking.

5. The initial position of the needle jet defined the position of the measurements relative to the wind tunnel and wing. The needle jet was removed before measurements were begun.

6. Flow was then started in the wind tunnel and the spectrum analyzers were adjusted for a spectrum width of 1 MHz/cm and the spectrum window was centered on the Doppler signal. The signals were then

played into the signal averager and stored, after which the tunnel operation ceased.

7. The maximum intensity point on each Doppler signal was then centered on the signal analyzer display and a frequency generator signal was played through each spectrum analyzer and the frequency corresponding to the mean Doppler frequency was hand recorded along with the position, spectrum width setting, tunnel static pressure, and air supply temperature.

8. The laser stand was then cranked in the Y direction to a new position and the data taking procedure repeated. The entire data taking procedure usually took from 3 to 5 minutes to accomplish.

Using the above procedure as many as 100 points on one profile could be taken in a day's time.

Although several profiles have been taken at the 7.0 downstream station only the data of April 21 and 22 are presented since this data is considered to be the most accurate and therefore provide the best representation of the flow at that station. The u, v and w components of velocity at that station are presented in Figures 20, 21 and 22, respectively. Although it was anticipated that this profile would pass very close to the core center, the data shows that the profile was below the core center. This can be noted in the behavior of the w velocity. If the measurements had been made directly across the core center, the w velocity component would be expected to be zero at the core center and have a characteristic shape similar to that sketched below.

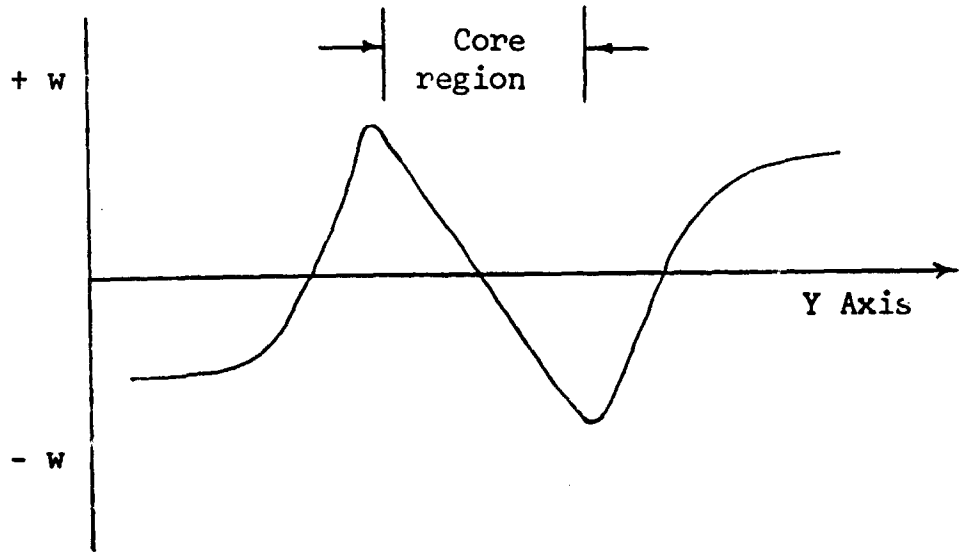

If the profile were above the core center, the w component would be positive and if below the core center, would be negative. The w component for the data presented is negative and, therefore, indicates that the profile is below the core center. Previous measurements at a z position that was 0.066 of an inch higher than the z position of the presented data showed that the w velocity component was positive, which indicated that the core center was located below that position. Assuming that the core position is stationary (the data of any particular profile indicates that this is the case), then the core center is located between Z = 0.00 and Z = 0.066" at the X = 7.00 " downstream station. Since neither of the profiles at either Z = 0.00" or Z = -0.066" give an indication that the core has been penetrated, it might be concluded that the core diameter is less than 0.066 inch. This diameter is much smaller than predicted by Speriter and Sacks (Reference 7). According to their analysis the diameter of the rolled up vortex for an elliptical wing loading, is given by the relation

$$d_c = .31s$$

where d_c = rolled up core diameter and s is the wing semi-span. For a wing semi-span of 3.5 inches the core diameter is 1.08 inches. This value is considerably larger than the measured data indicates. It might be noted that the predicted valu is for a completely rolled up vortex and the LDV measurements are at a downstream station where the vortex is not completely rolled up. Even so the predicted value is still unusually large in comparison. Speriter and Sacks provide further data from which the distance for vortex roll-up may be obtained. Using their data for the wing configuration used in the LDV measurements, a roll up distance of 7.96 inches is obtained. If this distance is correct, the roll-up process should be nearly complete at the X = 7.0 inch data presented. The data as well as the pictures of Figure 16 show the presence of a strong spiral which is a strong indication that the rolling up process is not yet completed. A more

complete picture of the rolling up process will be available when the data at the X = 14.0" station is analyzed.

One of the major problems in making comparisons of the data of Figures 20, 21 and 22 with that found in the literature is the presentation of coordinate systems. The experimental and theoretical data in the literature has the coordinate systems placed at the center of the vortex core and define the flow relations in terms of radial distances from the core center and the velocities at those positions (i.e. cyclindrical coordinates). The representation of the data in this form is quite logical, since the previous investigators consider the flow field only after the vortex has been formed and the spiraling and non-symmetry associated with the formation process is not considered.

Several attempts have been made to fit the LDV data into a coordinate system centered at the core center. Such efforts have not proved fruitful except from the standpoint of pointing up two characteristics of the data. One is that the flow field is in a definite spiral and the other is that unless the center of the spiral is known relative to the measured data positions, the spiral nature cannot be precisely defined. Although efforts to define this spiral are being made, no significant developments are presently available.

Several comparisons of the data have been made with the theoretical developments of Hoffman and Joubert (Reference 4) for turbulent line vortices. Their formulation applies mixing length theory to concentrically circular turbulent flow, along with dimensional analysis considerations, to arrive at the conclusion that for values of $VX/\Gamma_\infty > 150$ the vortex flow field is independent of viscosity. They further conclude that if this condition is met a universal tangential velocity profile exists which can be written in terms of radial position at which the peak tangential velocity occurs. This relation is given as

$$V = \frac{v(max)\ r(max)}{r} \left[1 + 2.14 \log_{10} \frac{r}{r(max)}\right]$$

For values of $r/r_{max} < 0.4$ V is defined by

$$V = \frac{1.83\ r^2}{r(max)}$$

Neglecting any spiral in the LDV data and assuming that the v velocity component represents the tangential velocity of a swirling symmetric vortex core, a comparison was made with a profile predicted by Hoffman and Joubert. This is shown in Figure 23. Their profile agrees surprisingly well with the LDV data. It is presently unclear as to why the agreement is so good, since the LDV data shows a clear indication that the flow field is in a spiral, and the unusually high w velocity presents the possibility of a very small core region (~ 0.06" diameter) and higher peak tangential velocities (~ 135-140 ft/sec).

It is anticipated that further analysis of the presently available data along with more measurements and analysis at X = 14.0" will help to clarify the present somewhat perplexing picture of the wing tip vortex flow field.

APPENDIX

Anticipated Results For Tube 3 On A Horizontal Traverse

Anticipated results have been computed for tube 3 in a Horizontal traverse for the orientation shown which has the laser beam normal to the pipe axis (along the Z axis) and tube 3 in the X-Z plane at an angle α with the Z axis.

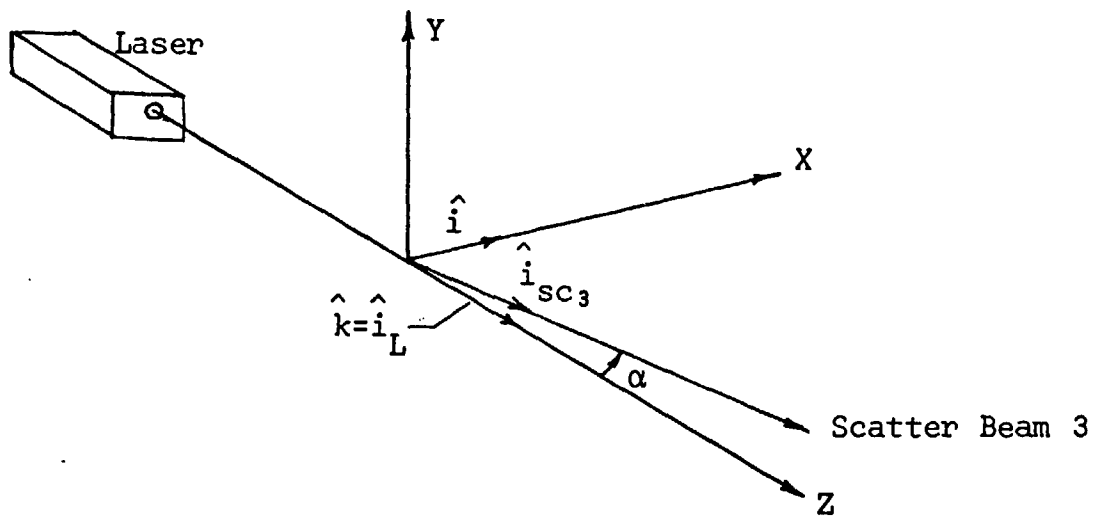

A unit vector along beam 3 is

$$\hat{i}_{sc_3} = \hat{i} \sin \alpha + \hat{k} \cos \alpha \qquad (1)$$

and the Doppler frequency shift f_3 is

$$f_3 = |(\hat{i}_{sc_3} - \hat{i}_L) \cdot \vec{V}|/\lambda \qquad (2)$$

With the velocity vector defined as

$$\vec{V} = u\,\hat{i} + v\,\hat{j} + w\,\hat{k} \qquad (3)$$

equation (21) becomes

$$\lambda f_3 = |\, u \sin \alpha + w\,(\cos \alpha - 1)| \qquad (4)$$

For the pipe turbulence test under consideration u>w and sin α > (cos α-1), so the absolute value can be omitted. Substituting a calibration constant A_3 to relate the frequency tracker output, e_3 to the frequency wavelength product,

$$A_3 = \lambda f_3 / e_3 \tag{5}$$

equation (4) because

$$A_3 e_3 = u \sin \alpha + w (\cos \alpha - 1) \tag{6}$$

To relate the velocity components shown to those normally reported, the velocity components and tracker voltage are assumed to consist of mean and fluctuating components.

$$\begin{aligned} u &= \bar{u} + u' \\ w &= \bar{w} + w' \\ e &= \bar{e} + e' \end{aligned} \tag{7}$$

The $\bar{w}$ component is assumed to be zero for the proposed test and LDV arrangement. Substituting equations (7) in (6) the following two relations are obtained.

$$A_3 \bar{e}_3 = \bar{u} \sin \alpha \tag{8}$$

$$A_3 e'_3 = u' \sin \alpha + w' (\cos \alpha - 1) \tag{9}$$

The first of these equations directly relates the mean velocity with the mean (or D.C.) tracker output, but the second equation must be reduced to an RMS voltage to be useful in comparing with the tracker output.

Squaring both sides of equation (9) and taking the time mean gives

$$A_3 \sqrt{\overline{e'^2_3}} = \sqrt{\sin^2 \alpha \, \overline{u'^2} + (\sin \alpha)(\cos \alpha - 1) \, \overline{u'w'} + (\cos \alpha - 1)^2 \, \overline{w'^2}} \tag{10}$$

For a horizontal traverse through the pipe centerline, the w' component is the radial component normally reported in the literature, so the right side of the equation can be evaluated from previous data.

The shear velocity which is used to nondimensionalize the turbulence components is

$$u_\tau = \overline{V}\sqrt{f/8} \qquad (11)$$

Where $\overline{V}$ = mass average velocity = 118 ft/sec

$f = 0.015$ for a smooth pipe at $Re = 25 \times 10^4$

Using the values shown for the proposed test

$u_\tau = 5.11$ ft/sec

For this value of a velocity, the following turbulence components are estimated from Laufer's data (Reference 1):

TABLE 1

r/Ro	$\sqrt{\overline{u'^2}}/u_\tau$	$\overline{u'^2}$	$\sqrt{\overline{w'^2}}/u_\tau$	$\overline{w'^2}$	$\overline{u'w'}/u_\tau^2$	$\overline{u'w'}$
0.0	0.80	16.709	0.73	13.913	0.0	0.0
0.2	0.92	22.097	0.77	15.479	0.2	5.221
0.4	1.14	33.929	0.85	18.863	0.4	10.443
0.6	1.38	49.719	0.95	23.562	0.6	15.664
0.8	1.65	71.077	1.02	27.162	0.8	20.886

NOTE: The w' component in this analysis is v' in Laufer's data.

The local value of $\overline{u}$ can be calculated from the velocity profile

$$u/U = ((Ro-r/Ro)^{1/n} \qquad (12)$$

Where: U = centerline velocity

$\overline{u}$ = local mean velocity at r

For a Reynolds Number of 250,000, n is approximately 7.65 (assuming $\overline{u}/U$ = 0.81 at r/Ro = 0.2, so the centerline velocity is:

$$U = \overline{V} \Big/ \frac{2n^2}{(n+1)(2n+1)}$$

$= 118/0.830$

$= 143$ ft/sec

Using this in equation (12) the following profile is obtained:

TABLE 2

r/Ro	$\bar{u}/U$	$\bar{u}$
0.0	1.000	142
0.2	0.971	138
0.4	0.935	133
0.6	0.887	126
0.8	0.810	115

Using the values in Tables 1 and 2 in equations (7) and (9) with a scattering angle, α, of 12° and 28° and an average A of 0.0252* ft/mv-sec, the following values are obtained:

TABLE 3

r/Ro	$A_3\sqrt{\overline{e'^2}}$	$A_3\overline{e}_3$	$\sqrt{\overline{e'^2}}$	$\overline{e}_3$	$\sqrt{\sin^2\alpha\,\overline{u'^2}}$	$\sqrt{\overline{e'^2} + 16}$
			(Millivolts)	(Volts)		(Millivolts)
(α =12°)						
0.0	0.8538	29.523	33.88	1.172	0.8499	34.11
0.2	0.9689	28.692	38.45	1.139	0.9773	38.66
0.4	1.1951	27.652	47.42	1.097	1.2110	47.59
0.6	1.4454	26.197	57.36	1.040	1.4660	57.50
0.8	1.7293	23.910	68.62	0.949	1.7528	68.74
(α = 28°)						
0.0	1.9678	66.664	78.09	2.645	1.919	78.19
0.2	2.1897	64.786	86.89	2.570	2.206	86.98
0.4	2.6763	62.439	106.20	2.477	2.734	106.27
0.6	3.2280	59.153	128.09	2.347	3.310	128.15
0.8	3.8587	53.989	153.12	2.142	3.957	153.17

The second and third columns of the tables give basic parameters which can be used to compute voltages for other values of A, while the fourth and fifth columns give voltages for the assumed value of A. The value listed in Column 6 is the result of solving equation (9) with w'=0. A comparison of this value with $A_3\sqrt{e_3'^2}$ shows that an error of 1 percent or less in $\sqrt{u'^2}$ would result if w' were assumed to be zero at α=12°. A higher error of 2.5 percent or less would result at a scattering angle of 28°. The voltage in column 7 is

* See next page

an indication of the effect of a 4 mv RMS noise level.

* Using $\lambda = .5145 \times 10^{-6}$ meters and e/f=67 MHz/mv

$$A = (0.5145 \times 10^{-6} \text{ meters} \times 3.28 \text{ ft/meters} \times 10^{6} \text{ 1/sec})\ 67 \text{ mv}$$

$$= 0.0252 \text{ ft/mv-sec}$$

REFERENCES

1. Laufer, John, "The Structure of Turbulence in Fully Developed Pipe Flow", NACA Report 1174, 1954

2. Coantie, Michel, "Contribution a l'Etude Theorique et Experimentale de l'Ecoulement Turbulent Dans un Tube Circularie," These, L'Universite d'Aix - Marseille, 1959.

3. Hooie, J. W., "An Experimental Investigation of Turbulent Pipe - Jets Near The Exit Plane", Thesis, Auburn University, Supervised by A. R. Barbin, 1965.

4. Hoffman, E. R. and Joubert, P. N., "Turbulent Line Vortices", J. Fluid Mech., Vol. 16, Part 3, July 1963, pp. 395-411

5. Newman, B. G., "Flow in a Viscous Trailing Vortex", The Aeronautical Quarterly, May 1959, pp. 149-162

6. Dosanjh, D. S., Gasparck, E. P. and Eskinazi, S., "Decay of a Viscous Trailing Vortex", The Aeronautical Quarterly, May 1962, pp 167-188.

7. Spreiter, John R., and Sacks, Alvin H., "The Rolling Up of the Trailing Vortex Sheet and Its Effect on the Downwash Behind Wings", J. Aero Sciences, Vol. 18. 1951.

8. McCormick, Barnes W. et al, "Structure of Trailing Vortices", J. of Aircraft, Vol. 5, No. 3, May-June 1968.

9. Fuller, C. E., "Development Testing and Application of a Three Dimensional Laser Doppler Velocimeter for the Measurement of Gas Flows", Hayes International Corp., Report No. 1678, April 1970.

FIGURE 1. PIPE TURBULENCE

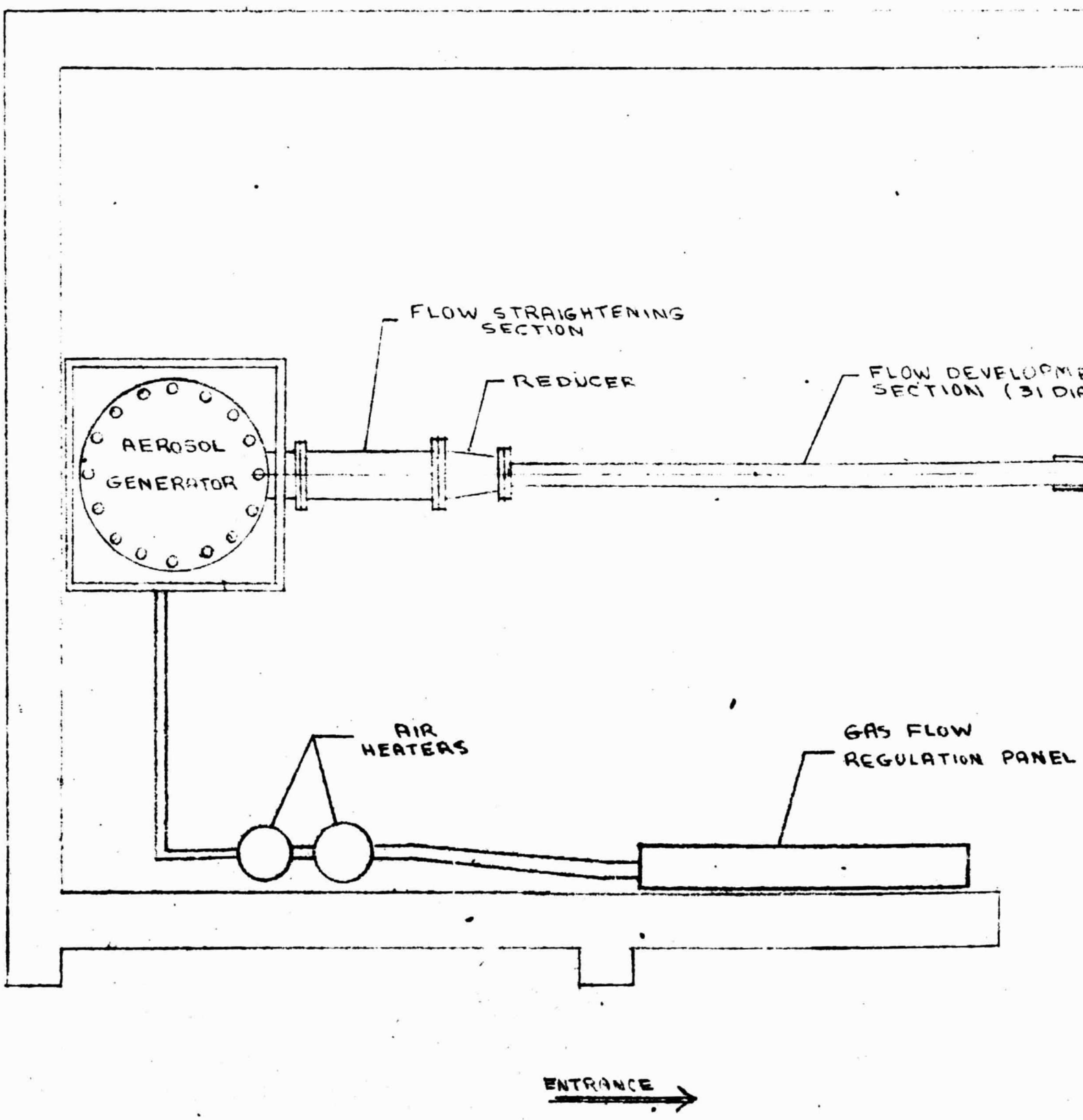

FOLDOUT FRAME

NASA/MSFC BUIL

E TEST ARRANGEMENT

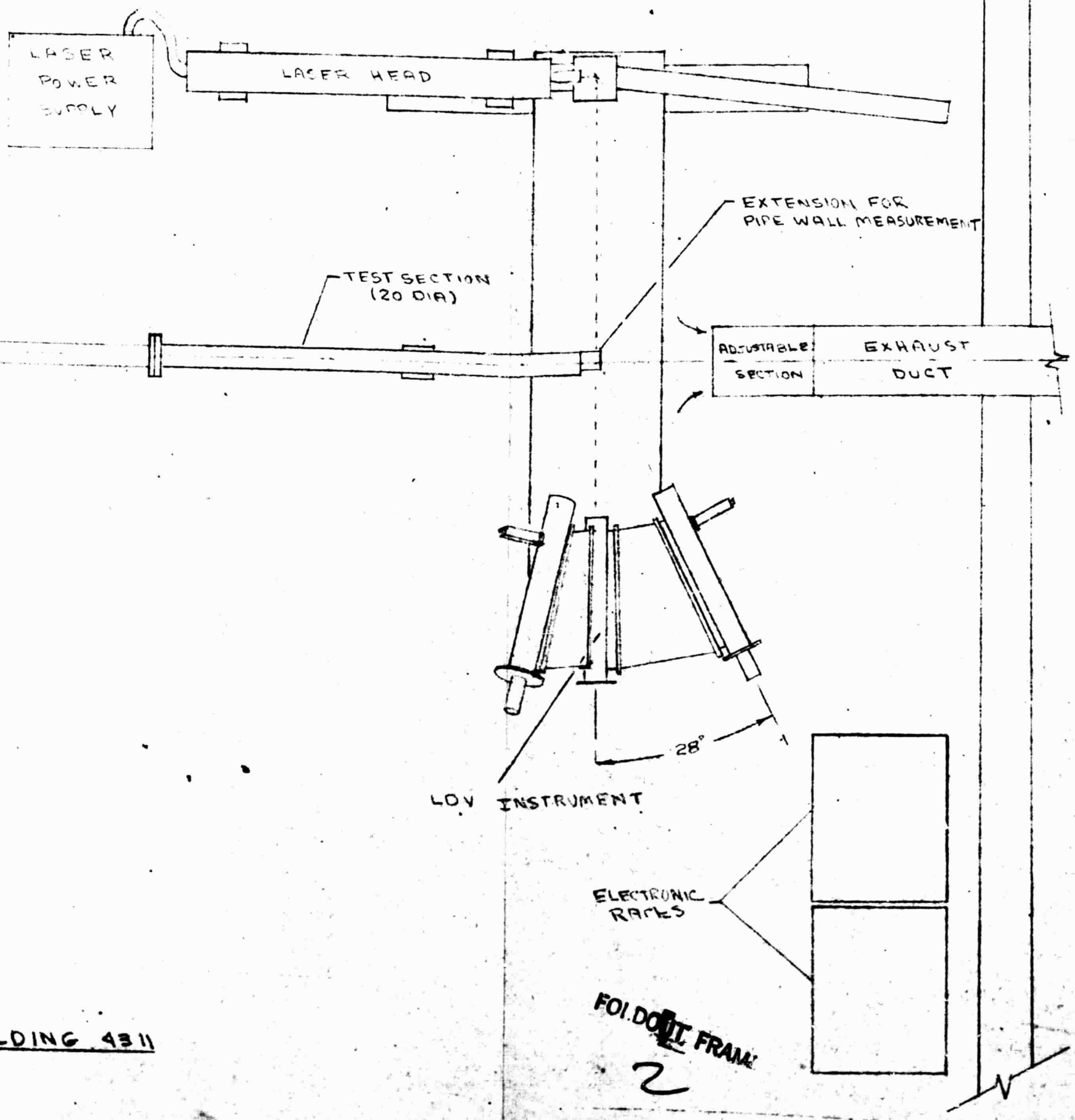

2

LDING 9311

SEC.
10'
(3

HONEYCOMB

REDUCER

SANDPAPER ROUGHNESS
3 DIAMETERS LONG

SCREENS

CONNECTED TO
AEROSOL GENERATOR

5' APPROX

FOLDOUT FRAME

7'

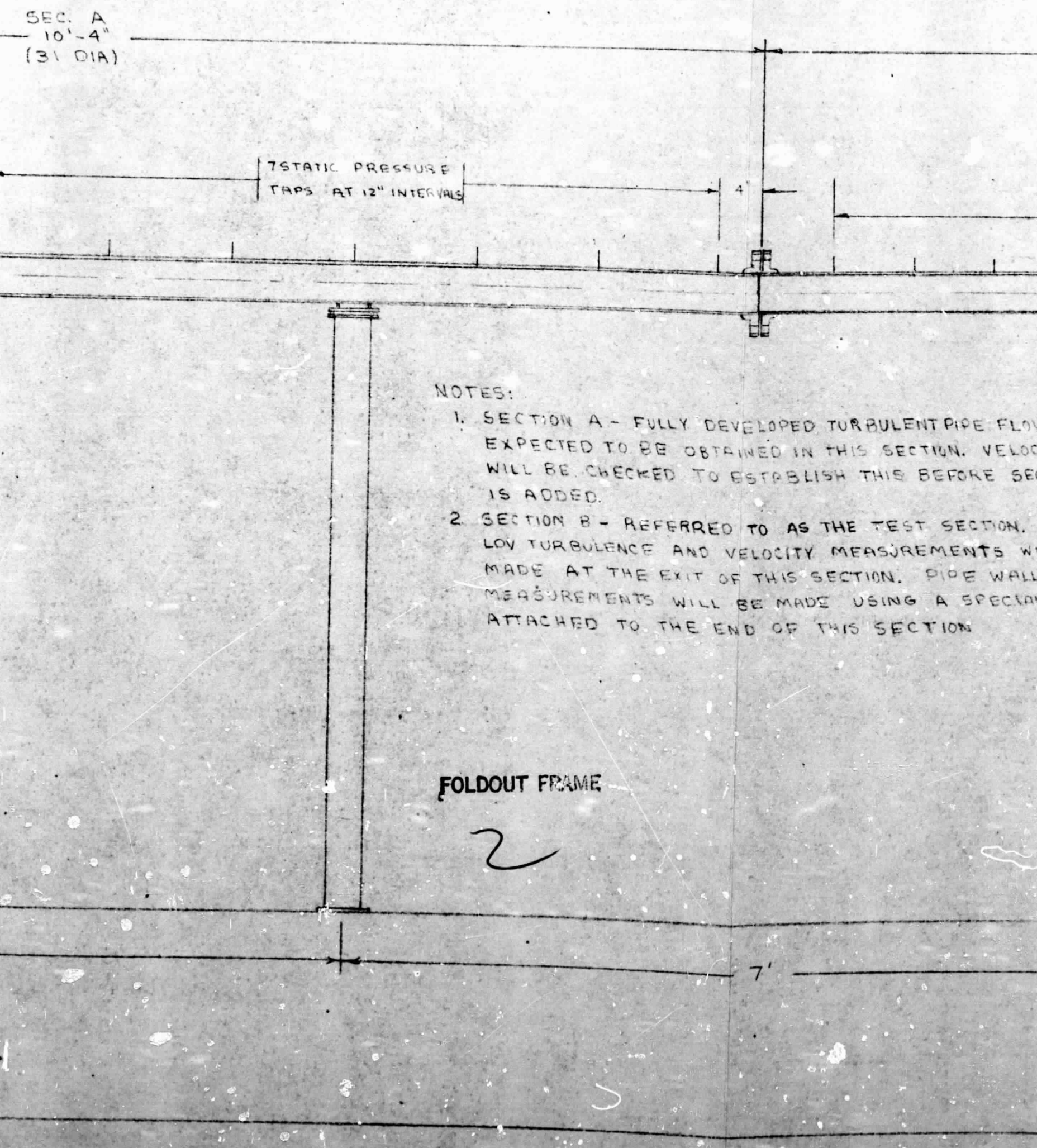

NOTES:

1. SECTION A - FULLY DEVELOPED TURBULENT PIPE FLO
EXPECTED TO BE OBTAINED IN THIS SECTION. VELOC
WILL BE CHECKED TO ESTABLISH THIS BEFORE SE
IS ADDED.
2. SECTION B - REFERRED TO AS THE TEST SECTION.
LDV TURBULENCE AND VELOCITY MEASUREMENTS W
MADE AT THE EXIT OF THIS SECTION. PIPE WALL
MEASUREMENTS WILL BE MADE USING A SPECIA
ATTACHED TO THE END OF THIS SECTION

FOLDOUT FRAME

2

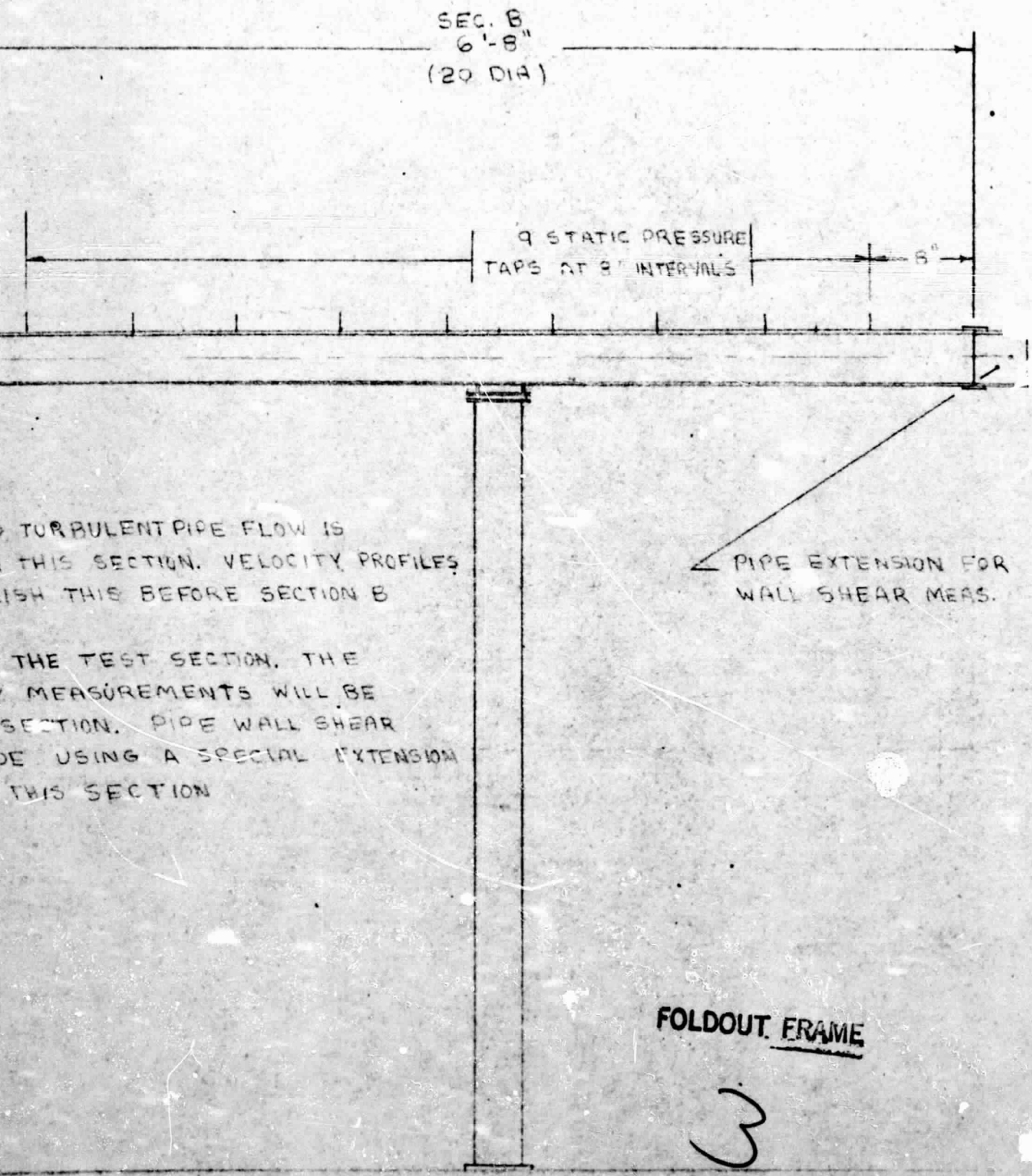

FOLDOUT FRAME

3

FIGURE 2 DETAIL OF PIPE ARRANGEMENT FOR LDV PIPE TURBULENCE TEST

PRECEDING PAGE BLANK NOT FILMED

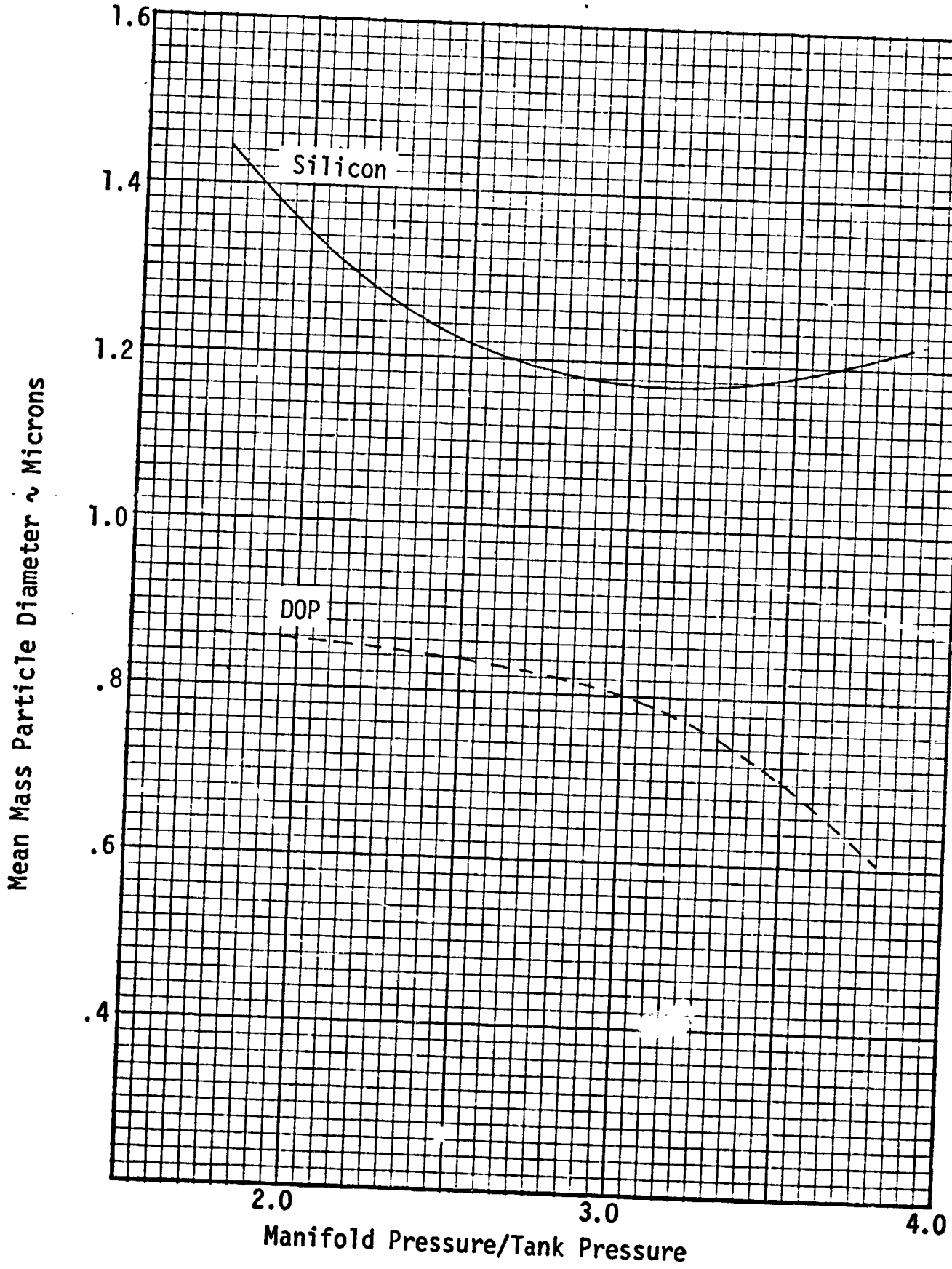

FIGURE 3 MEAN PARTICLE DIAMETERS EXPECTED FOR DIFFERENT OPERATING PRESSURE RATIOS

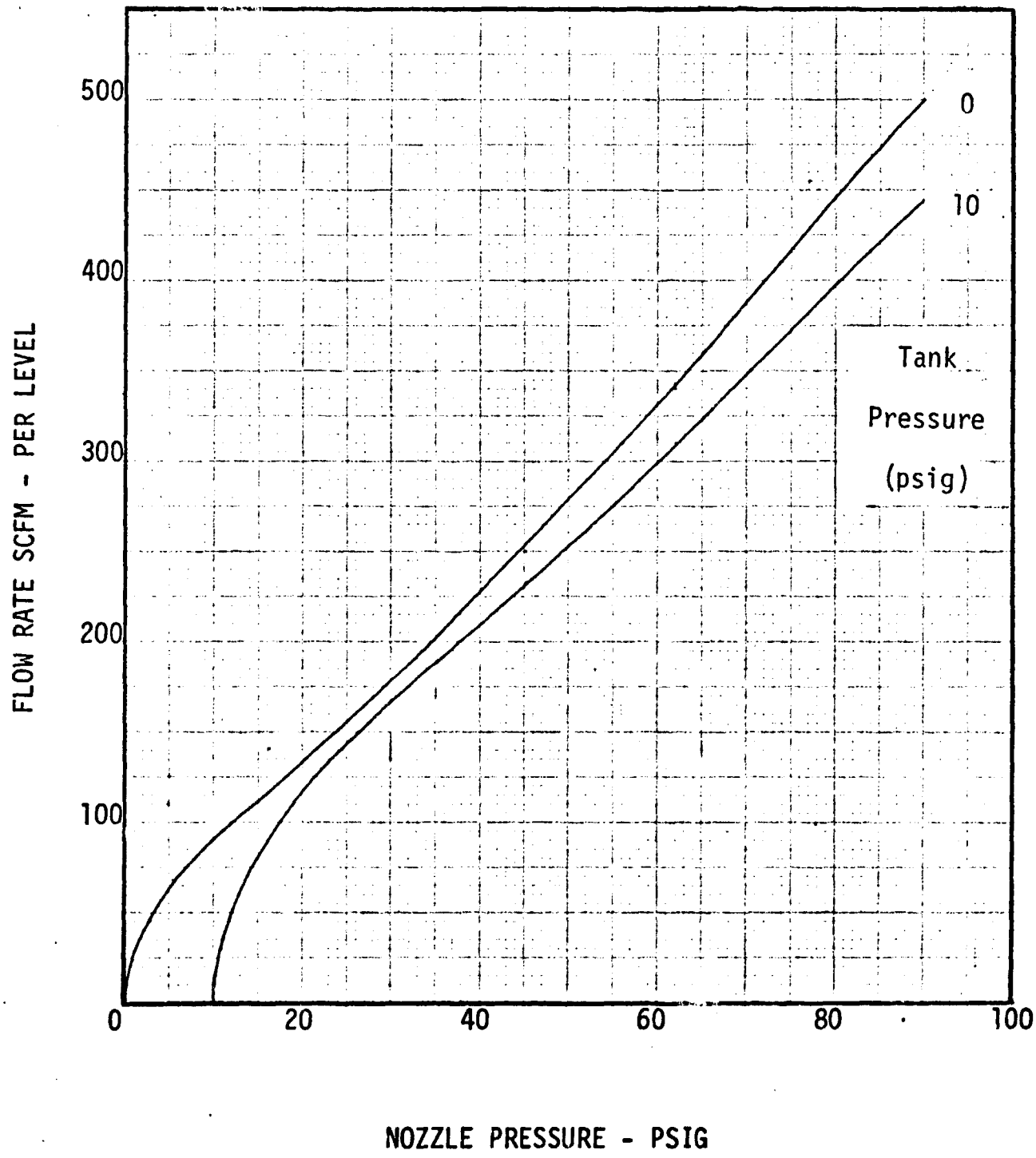

Figure 4 Expected Aerosol Generator Flow Rate Per Level for Different Operating Pressures.

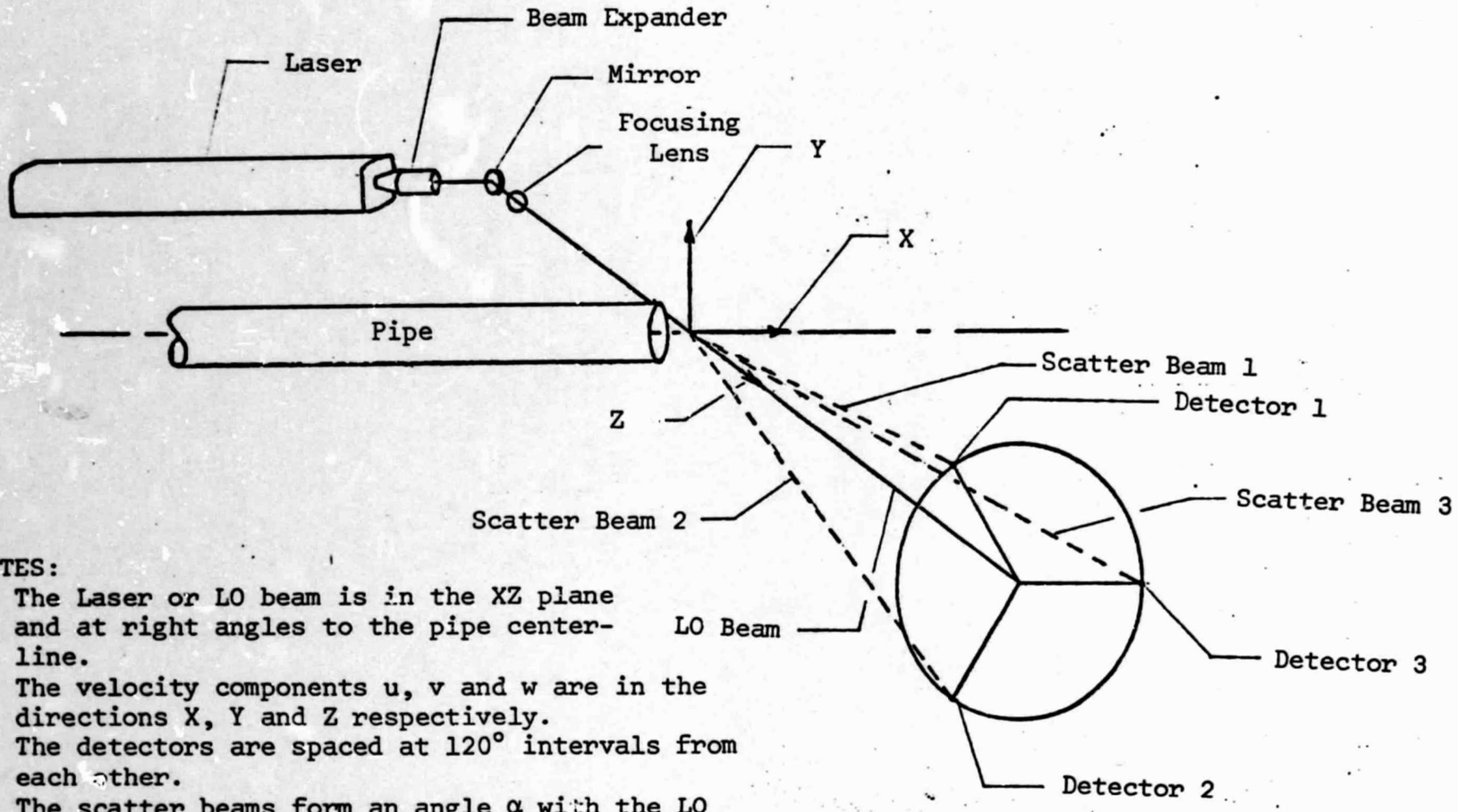

NOTES:

1. The Laser or LO beam is in the XZ plane and at right angles to the pipe centerline.
2. The velocity components u, v and w are in the directions X, Y and Z respectively.
3. The detectors are spaced at 120° intervals from each other.
4. The scatter beams form an angle α with the LO beam. This angle can be set at either 8.5°, 12°, 18° or 28°.
5. The plane formed by scatter beam 3 and the LO beam lies parallel to the pipe centerline.

Figure 5 Schematic of the Three Dimensional Laser Doppler Velocimeter and its Angular Alignment Relative to the Pipe

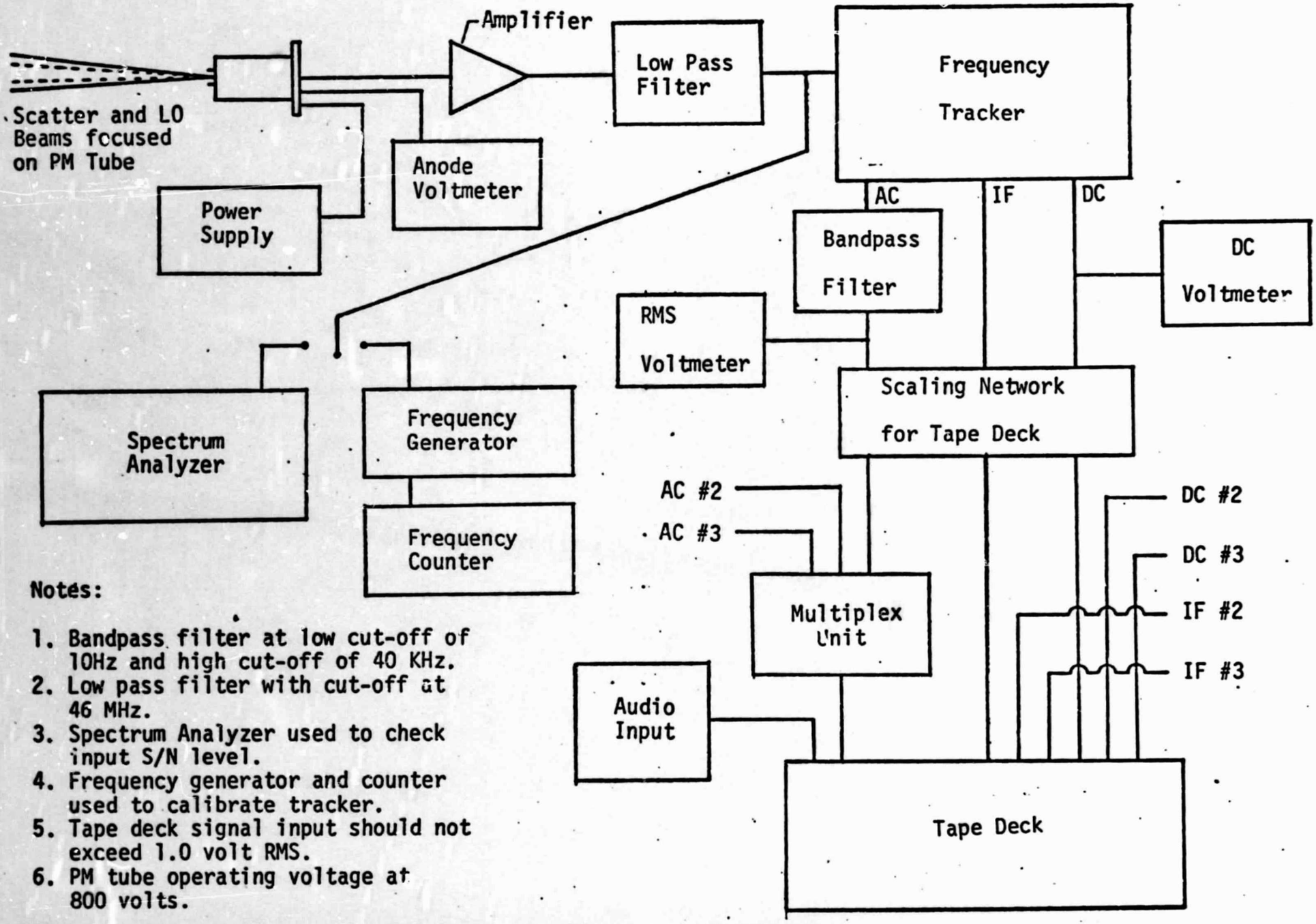

Notes:

1. Bandpass filter at low cut-off of 10Hz and high cut-off of 40 KHz.
2. Low pass filter with cut-off at 46 MHz.
3. Spectrum Analyzer used to check input S/N level.
4. Frequency generator and counter used to calibrate tracker.
5. Tape deck signal input should not exceed 1.0 volt RMS.
6. PM tube operating voltage at 800 volts.

Figure 6 Schematic of the LDV Electronic Network for the Pipe Turbulence Tests

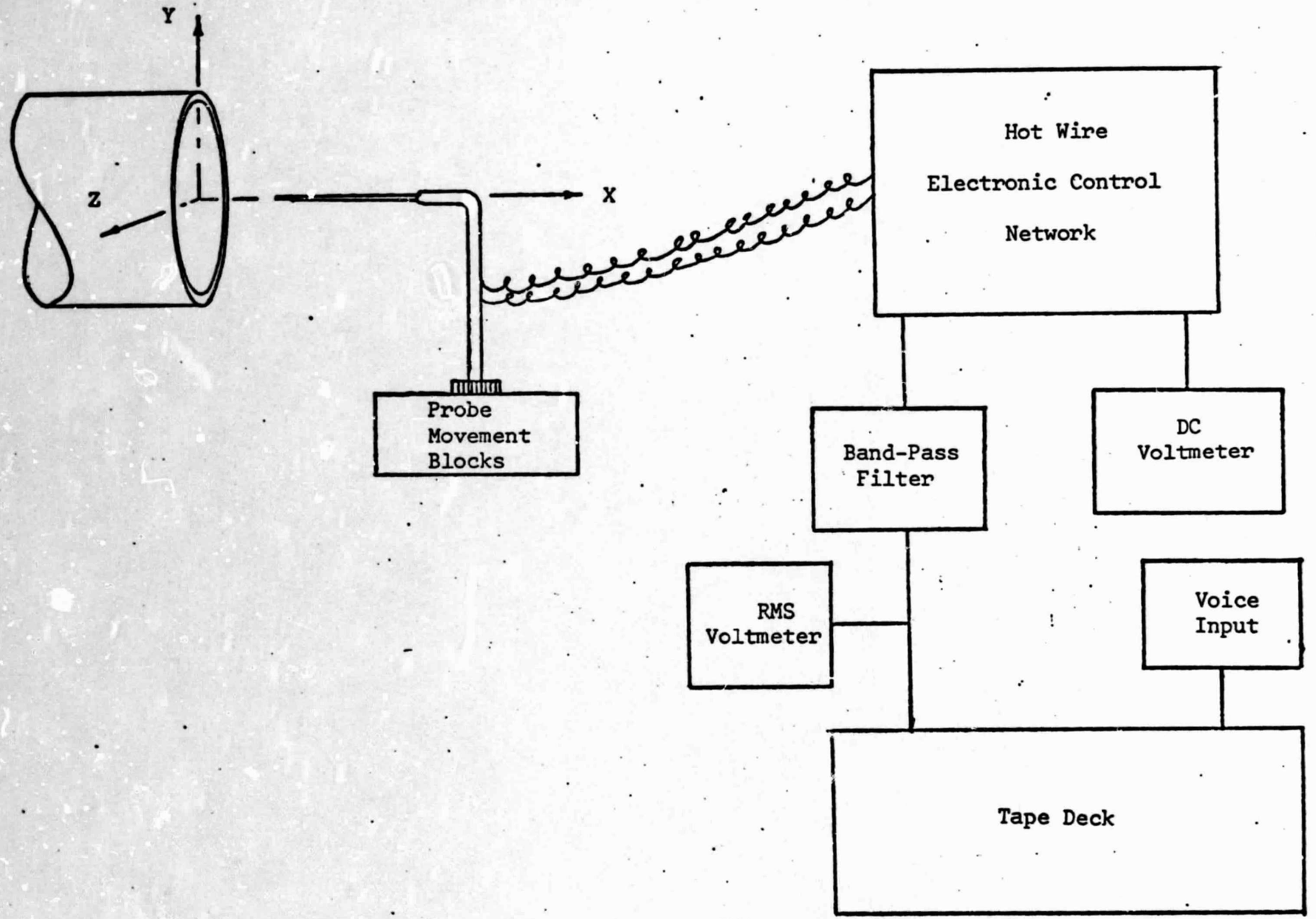

Figure 7 Sketch of Test Arrangement for Hot Wire Pipe Measurements

POSITION (Inches)			RECORDING METHOD*		REQUIRED FLOW DATA		
X	Y	Z	DC VOLTAGE	RMS VOLTAGE	$\overline{u'^2}$	U	FREQUENCY SPECTRUM
1.25	0.0	0.0	W	W,T	X	X	X
	.20			W	X	X	
	.40			W	X	X	
	.60			W,T	X	X	X
	.80			W	X	X	
	.90			W	X	X	
	1.00			W,T	X	X	X
	1.10			W	X	X	
	1.20			W,T	X	X	X
	1.30			W	X	X	
	1.40			W,T	X	X	X
	1.50			W	X	X	
	1.60			W,T	X	X	X
	1.70			W	X	X	
	1.80			W,T	X	X	X

*W - Written Recording
T - Tape Recording

TEST CONDITIONS

Centerline Exit Velocity	143 ft/sec (4.612 in H_2O)
Flow Temperature	70° F
Overheat Ratio	1.4
Low Frequency Cut-Off	10 Hz
High Frequency Cut-Off	40 KHz
Pressure on 5 opened Generator Nozzles	51.2 psig

FIGURE 8 Hot Wire Data Required For Pipe Turbulence Test

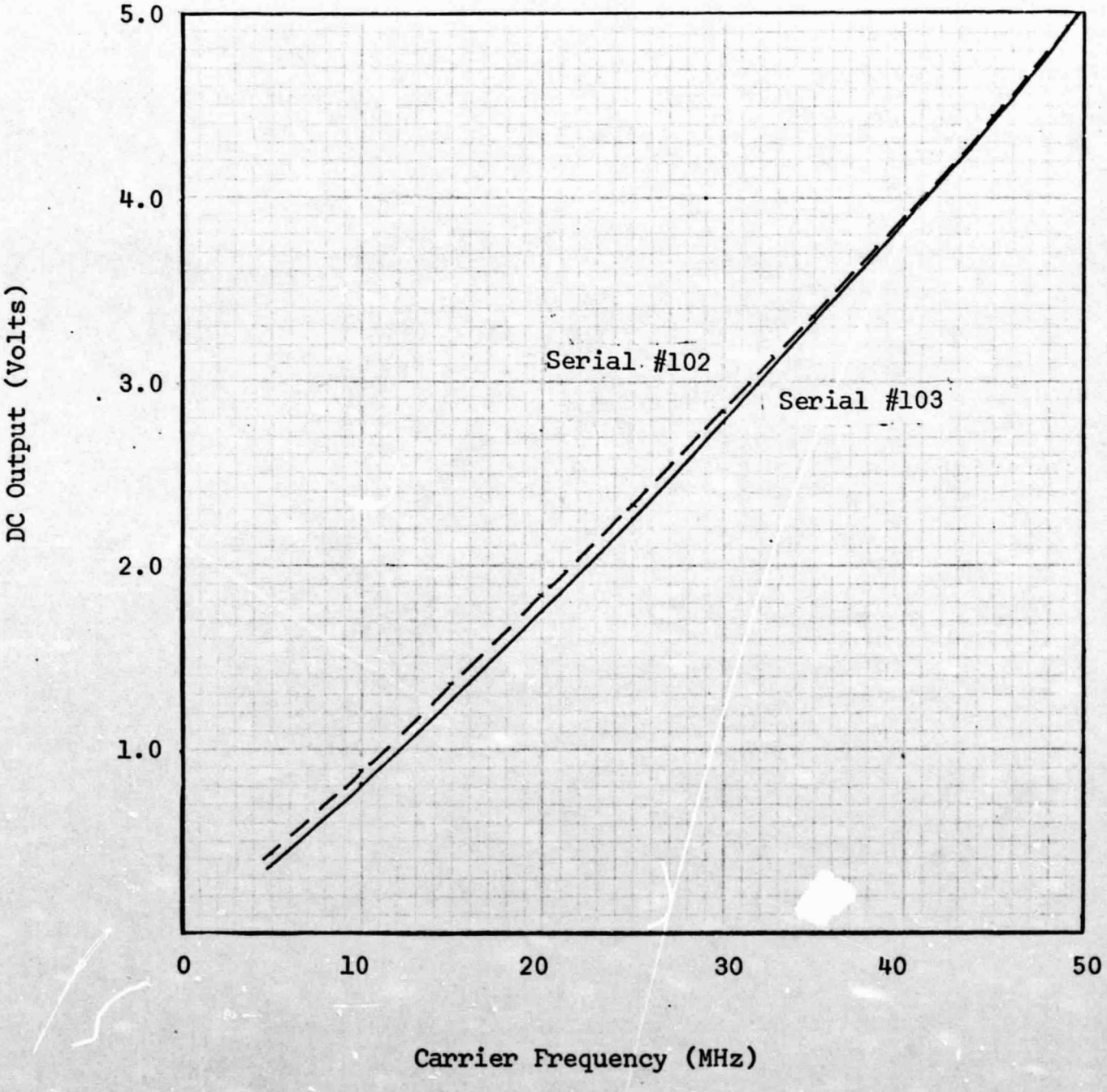

Figure 9 DC Calibration for Frequency Trackers with Serial Numbers 102 and 103.

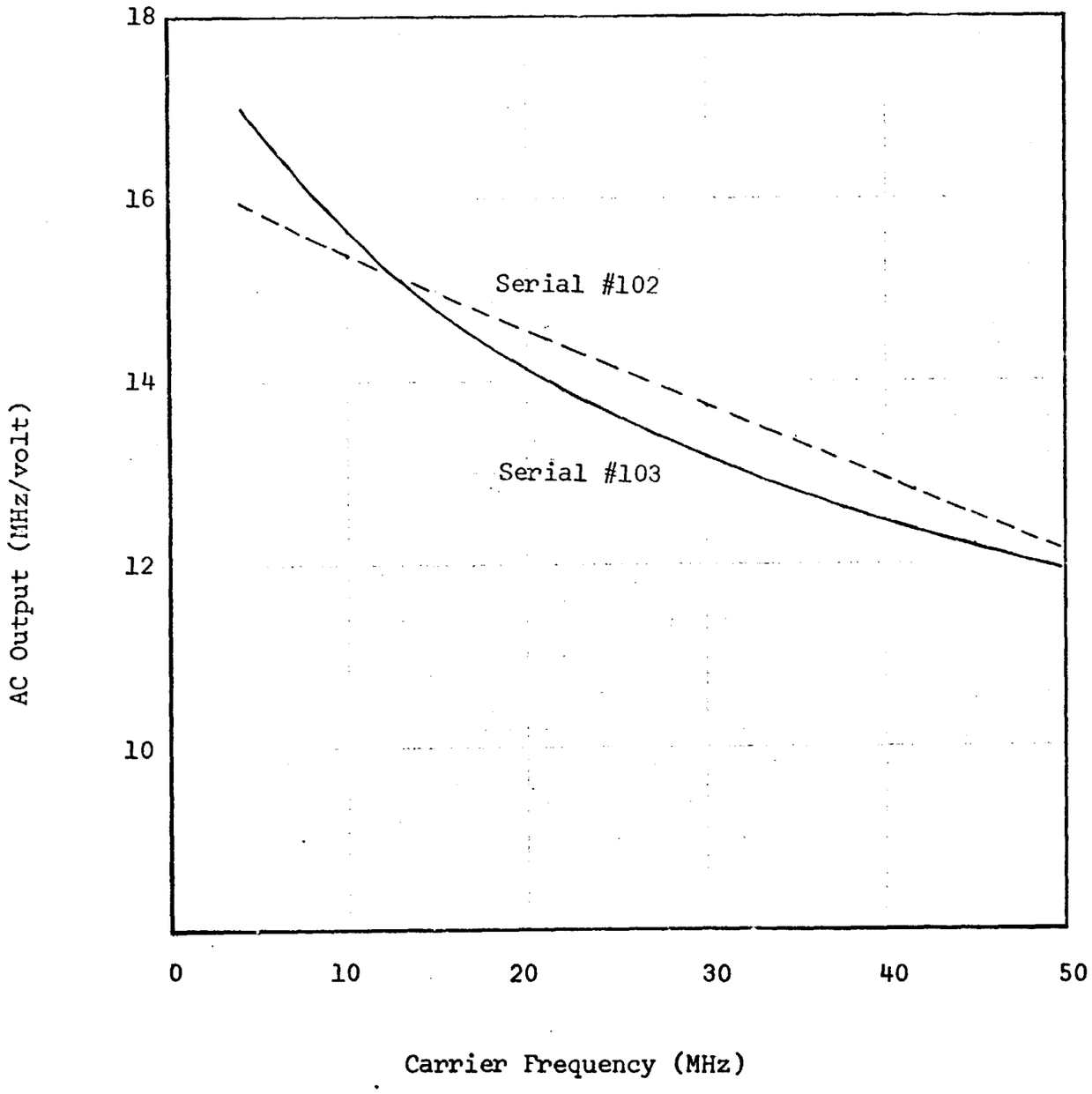

Figure 10 AC Calibration for Frequency Trackers with Serial Numbers 102 and 103.

POSITIONS (Inches)			RECORDING METHOD*			REQUIRED FLOW DATA						
X	Y	Z	DC VOLTAGE	AC VOLTAGE	IF DET	$\overline{u'^2}$	$\overline{u'^2}$	$\overline{w'^2}$	$\overline{u'v'}$	$\overline{u'w'}$	$\overline{v'w'}$	Frequency Spectra u,v & w
1.25	0.0	0.0	W, T	W, T	T	X	X	X	X	X	X	X
	.20											
	.40											
	.60											X
	.80											
	.90											X
	1.00											
	1.10											X
	1.20											
	1.30											X
	1.40											
	1.50											X
	1.60											
	1.70											X
	1.80											

* W - Written Recording
T - Tape Recording

NOTE: See Figure 11a for Test Conditions

FIGURE 11 LDV Data Points for Pipe Turbulence Test

TEST CONDITIONS

Centerline Exit Velocity	143 ft/sec (4.612 in H_2O)
Flow Temperature	70° F
Particle Concentration	>10^6 Particles/cm^3
Mean Particle Size	>1.0 Micron
Low Frequency Cut-Off	10 Hz
High Frequency Cut-Off	40 KHz
Tracker Mode	Wide
Laser Power	1.6 Watts
P.M. Voltage	800 Volts
Scatter Angle	28° at X = 1.25
Expected Centerline Doppler Frequency	28° - #1 (14.15 MHz), #2 (14.15 MHz), #3 (28.30 MHz)

NOTE: See Figure 11 LDV Data Points for Pipe Turbulence Test

FIGURE 11a LDV Data Conditions for Pipe Turbulence Test

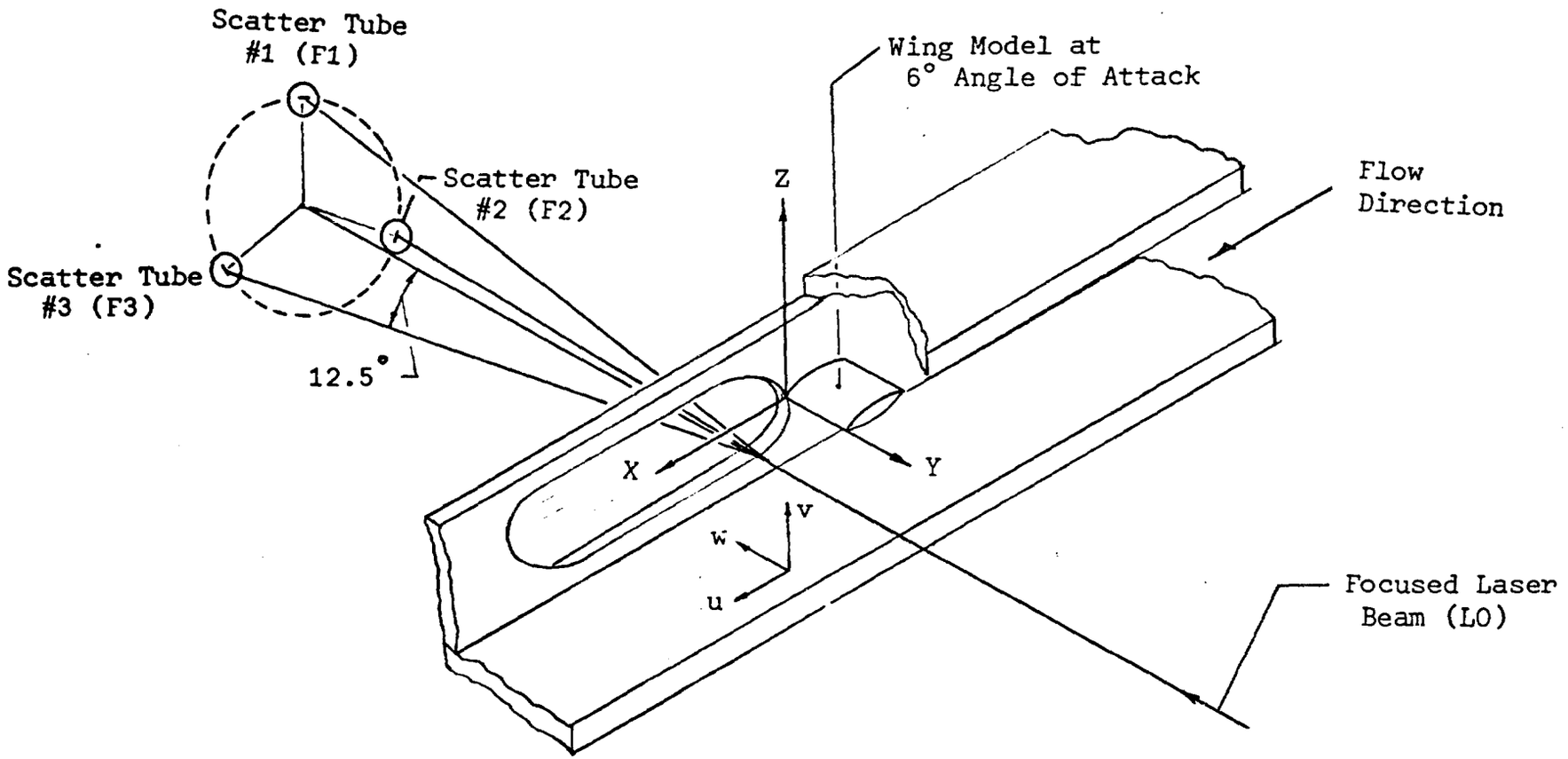

Figure 12. Sketch of LDV Instrumentation Arrangement Relative to Tunnel Coordinate System

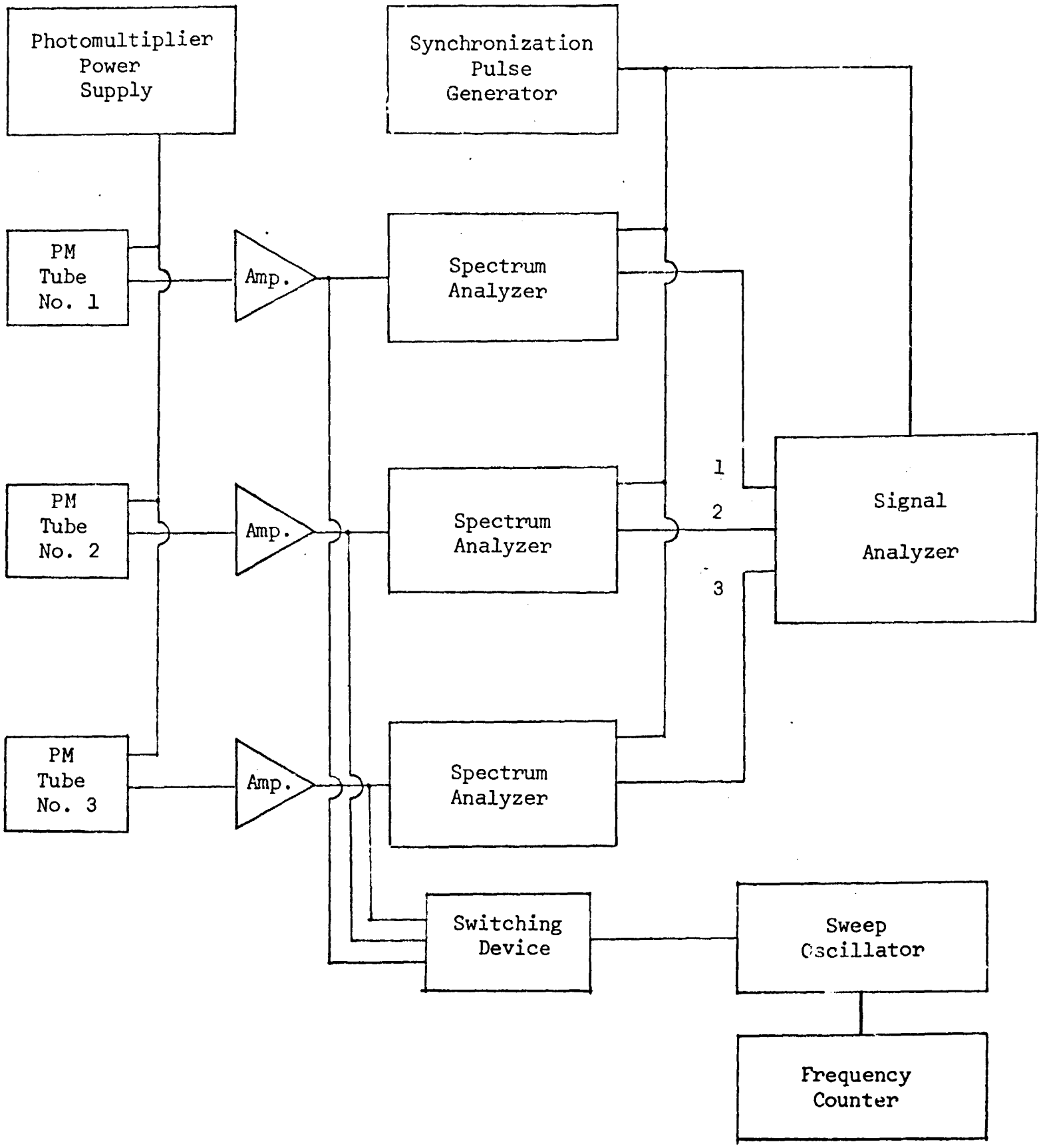

Figure 13 Schematic of Electronic Network for Data Acquisition and Identification at the MSFC 7 x 7-Inch Wind Tunnel Tests

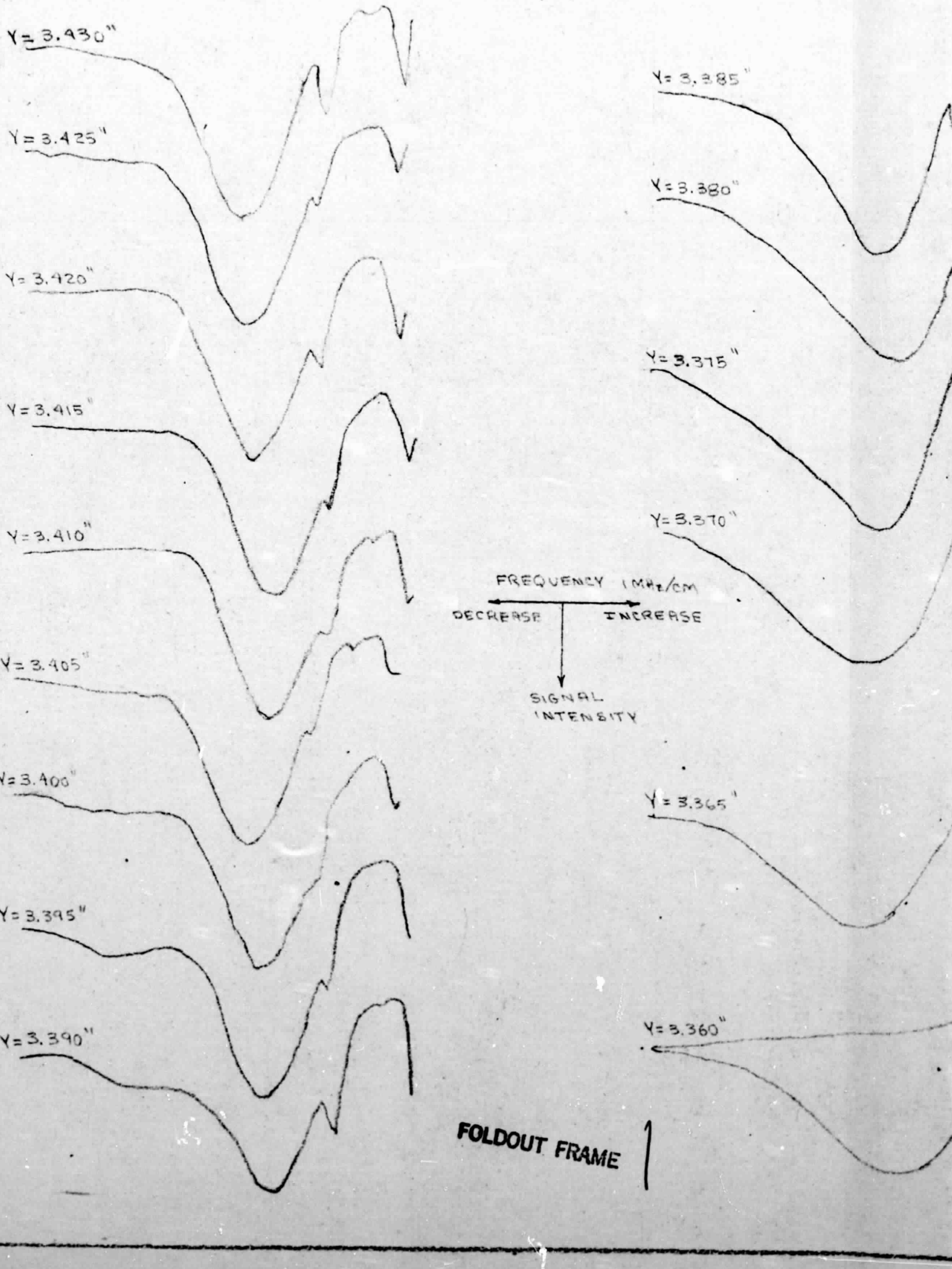

FOLDOUT FRAME 1

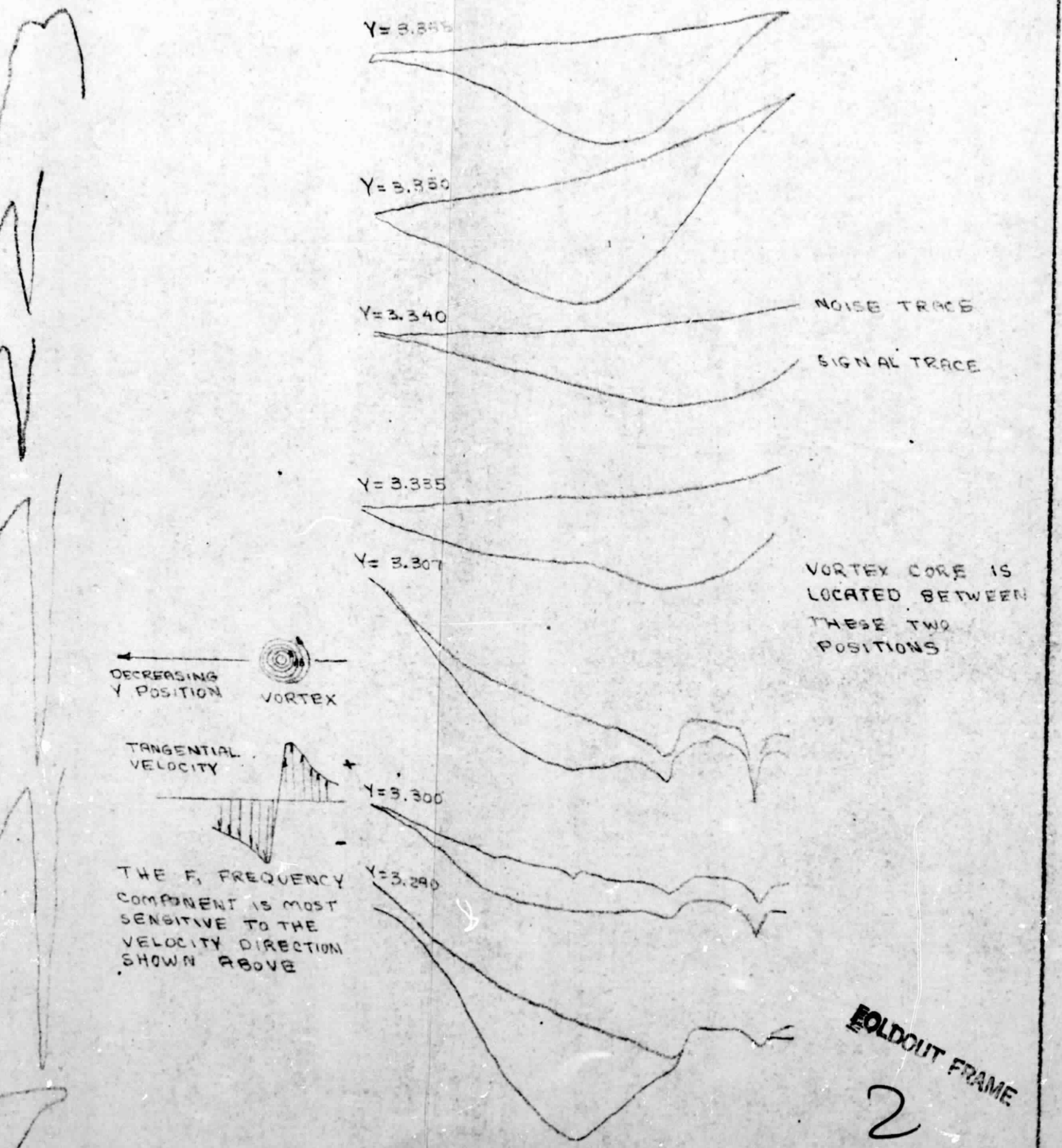

FIGURE 14 DOPPLER SPECTRUM TRACES FOR F_1 SIGNAL COMPONENT AT POSITIONS ON EITHER SIDE OF THE VORTEX CORE REGION - 7 INCHES FROM WING TRAILING EDGE

Date	Position X	Z	Y Position From	To	No. Data Points Measured
2-16-71	7.000	0.0	4.500	4.500	6
2-17-71	7.00	0.0	4.50	0.75	17
2-22-71	7.00	0.0	4.50	3.110	45
2-25-71	7.00	0.0	4.50	2.80	55
3-11-71	7.00	0.0	5.5	4.50	7
3-12-71	7.00	0.0	5.5	2.60	47
3-17-71	7.00	0.0	4.5	3.23	54
3-18-71	7.00	0.0	3.5	3.185	26
3-25-71	7.00	0.0	3.5	2.835	41
4-13-71	7.00	-0.066	4.5	3.430	27
4-21-71	7.00	-0.066	4.5	3.200	60
4-22-71	7.00	-0.066	4.5	0.30	114
4-27-71	14.0	-0.066	5.5	3.040	93
5-19-71	14.0	+0.067	5.5	0.50	110
5-20-71	14.0	+0.189	5.5	0.50	95

NOTE: Free stream velocity 278 ft/sec.

Figure 15 Vortex Data Measurement Positions.

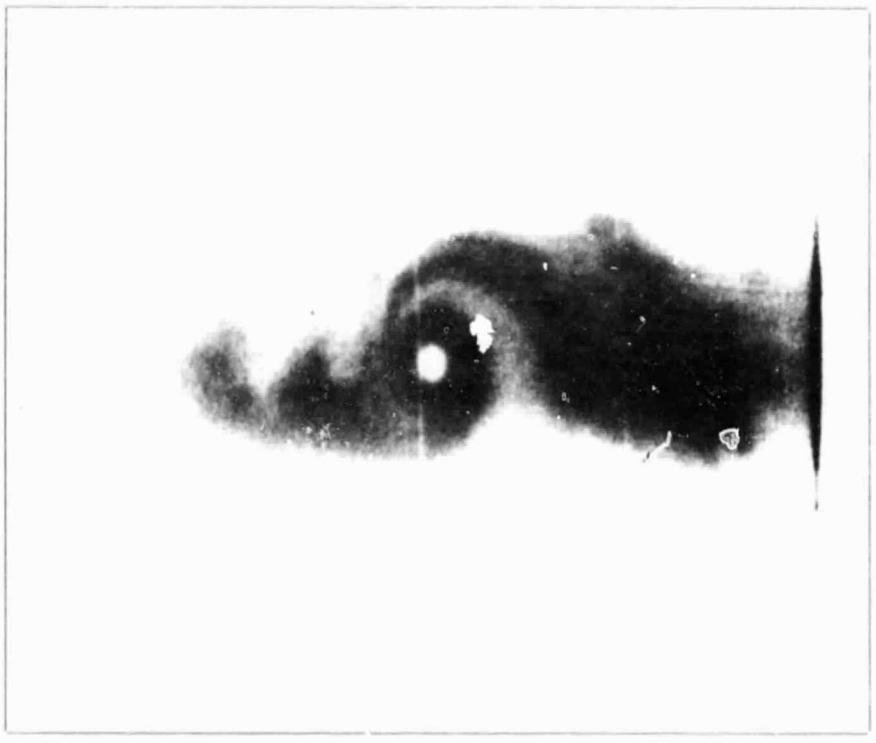

Figure 16 Visual Display of Wing Tip Vortex Pattern in MSFC 7 X 7 Inch Wind Tunnel at 7 Inch Downstream of Wing Trailing Edge.

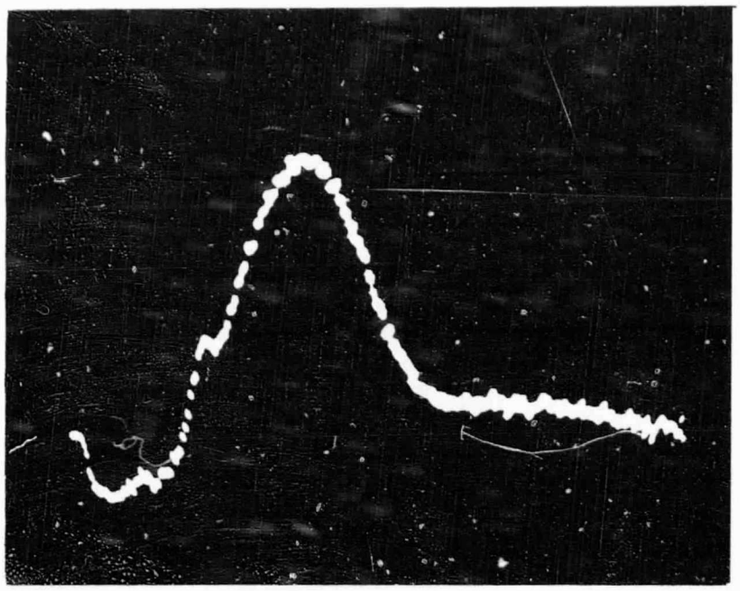

Signal Trace Outside Core Region.

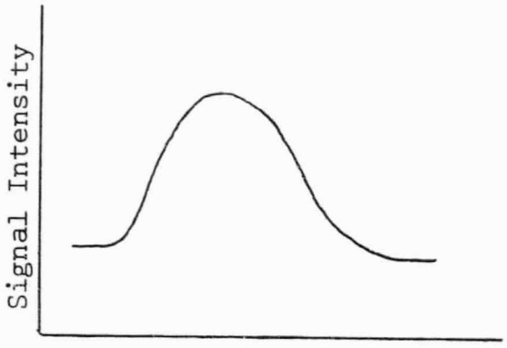

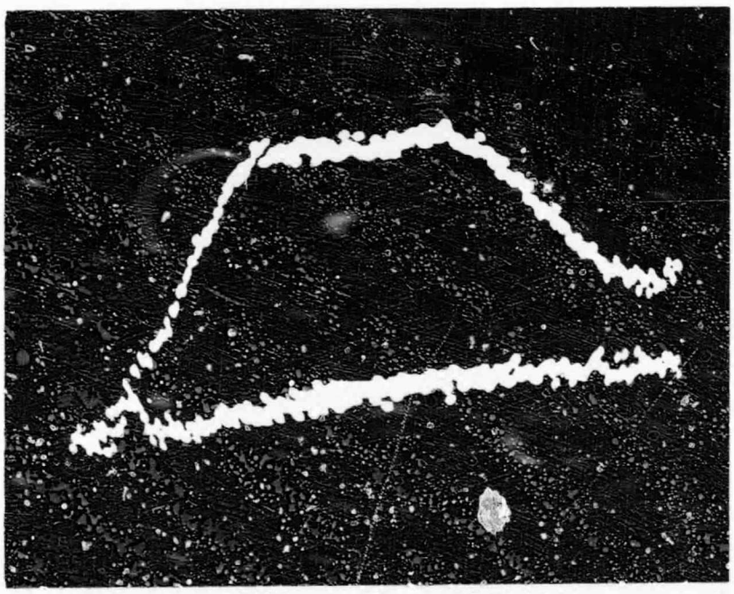

Signal and Noise Trace Close to Core - Note the Broadness.

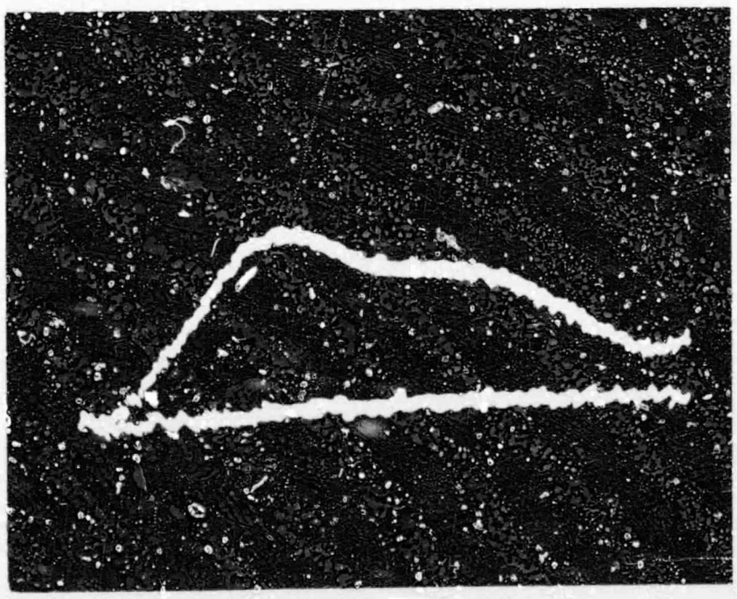

Signal and Noise Trace Slightly Closer to Core - Note Amplitude Reduction and Double Hump Nature of Signal.

Figure 17 Doppler Frequency Spectrums of F_1 Component Showing Changes at Points Close to the Vortex Core.

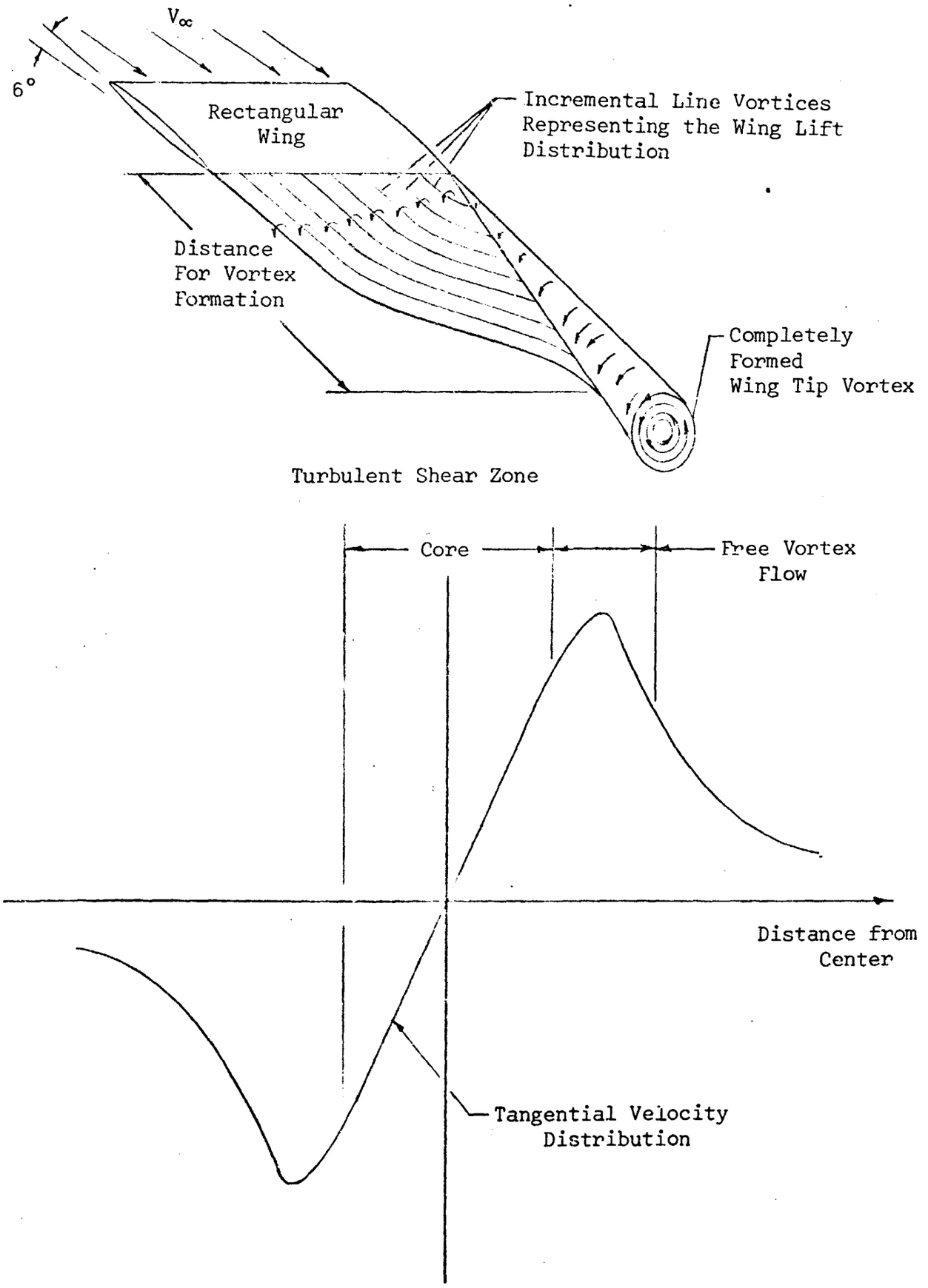

Figure 18 Schematic Representation of Wing Tip Vortex Formation and the Vortex Model Based on Tangential Velocity Distribution.

Figure 20 Variation in the u Velocity Component in a Wing Tip Trailing Vortex in MSFC 7 Inch Wind Tunnel

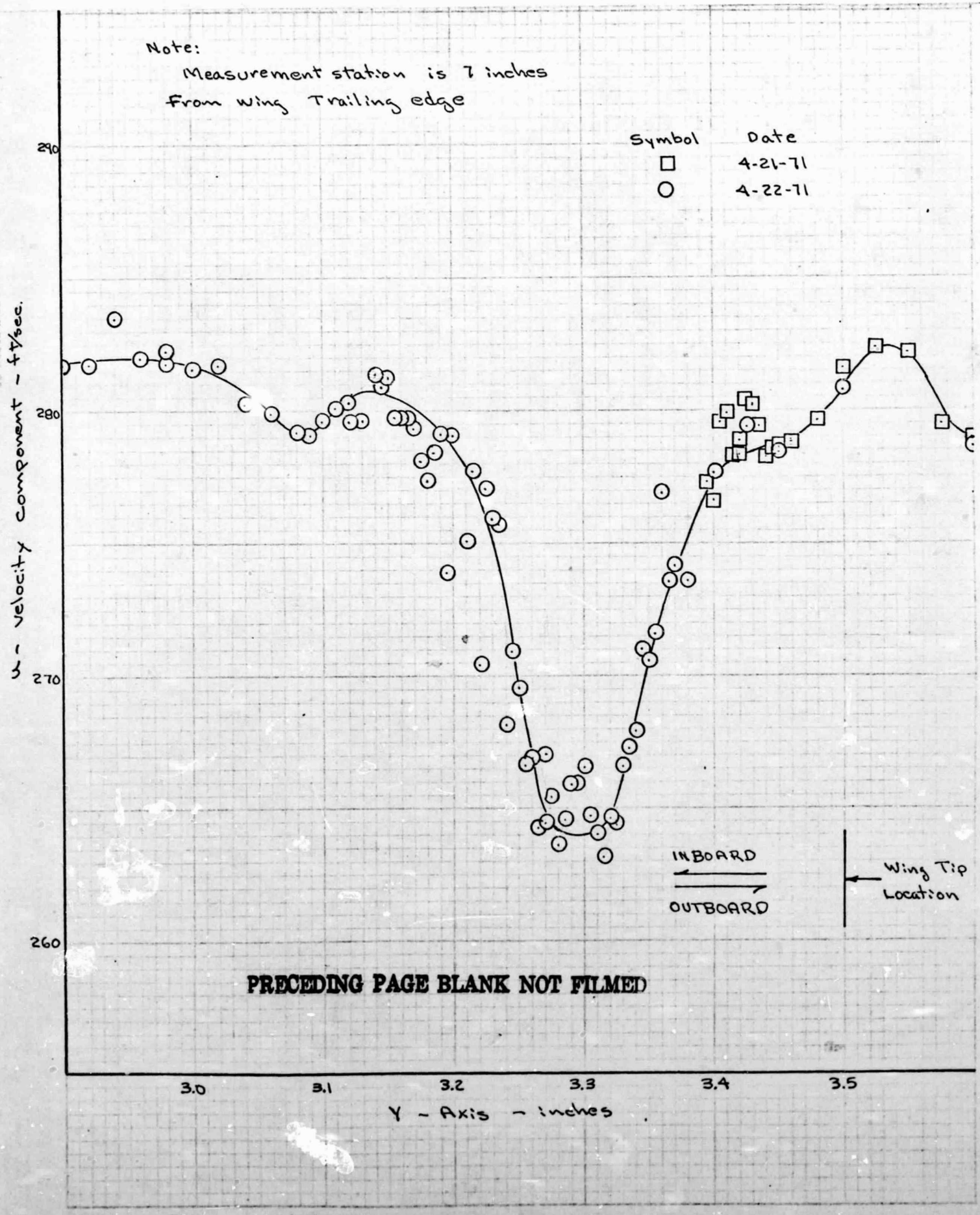

PRECEDING PAGE BLANK NOT FILMED

Figure 21 Variation in the v Velocity Component in a Wing Tip Trailing Vortex in MSFC 7 Inch Wind Tunnel

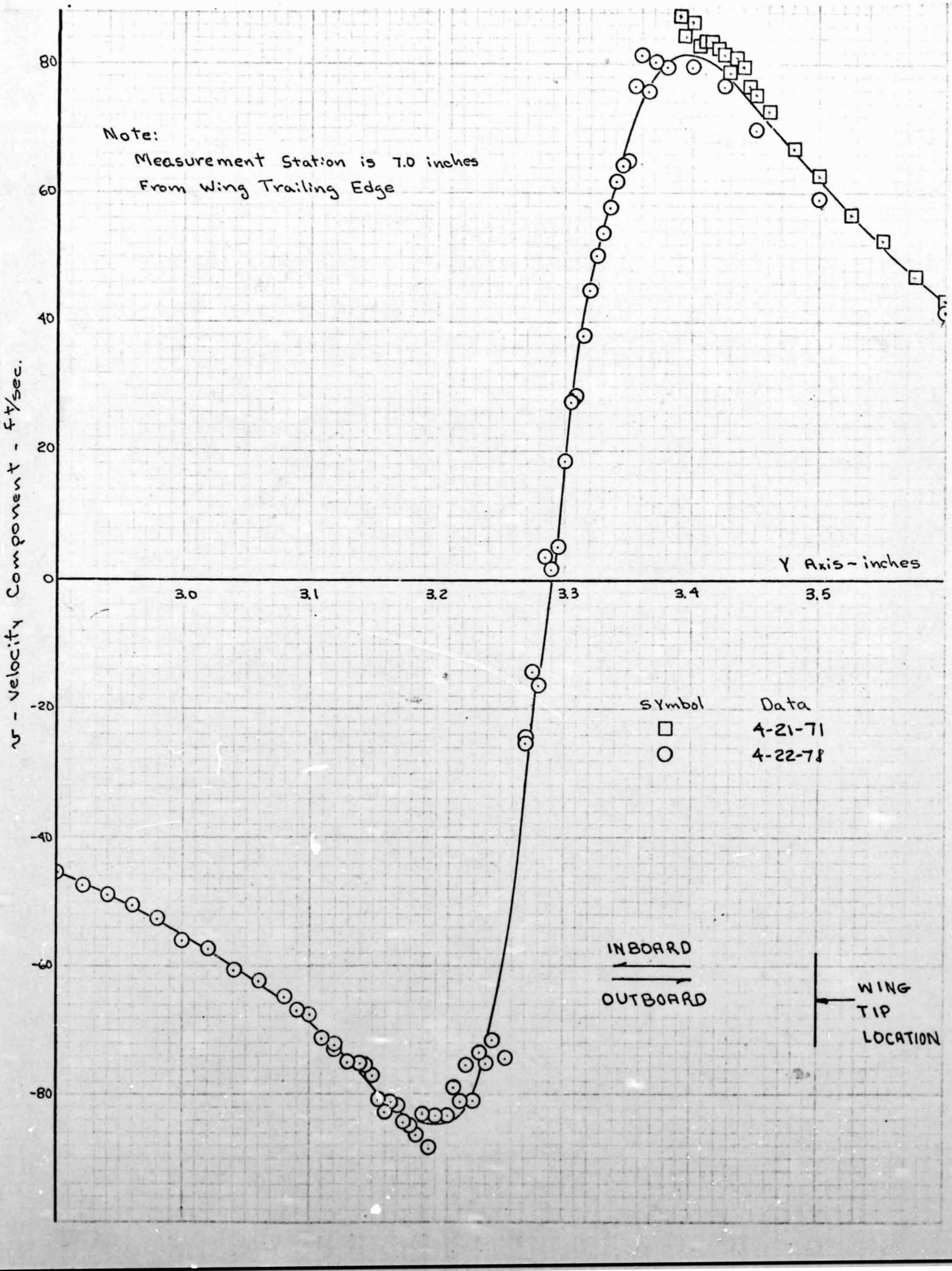

Figure 22 Variation in the w Velocity Component in a Wing Tip Trailing Vortex in MSFC 7 Inch Wind Tunnel

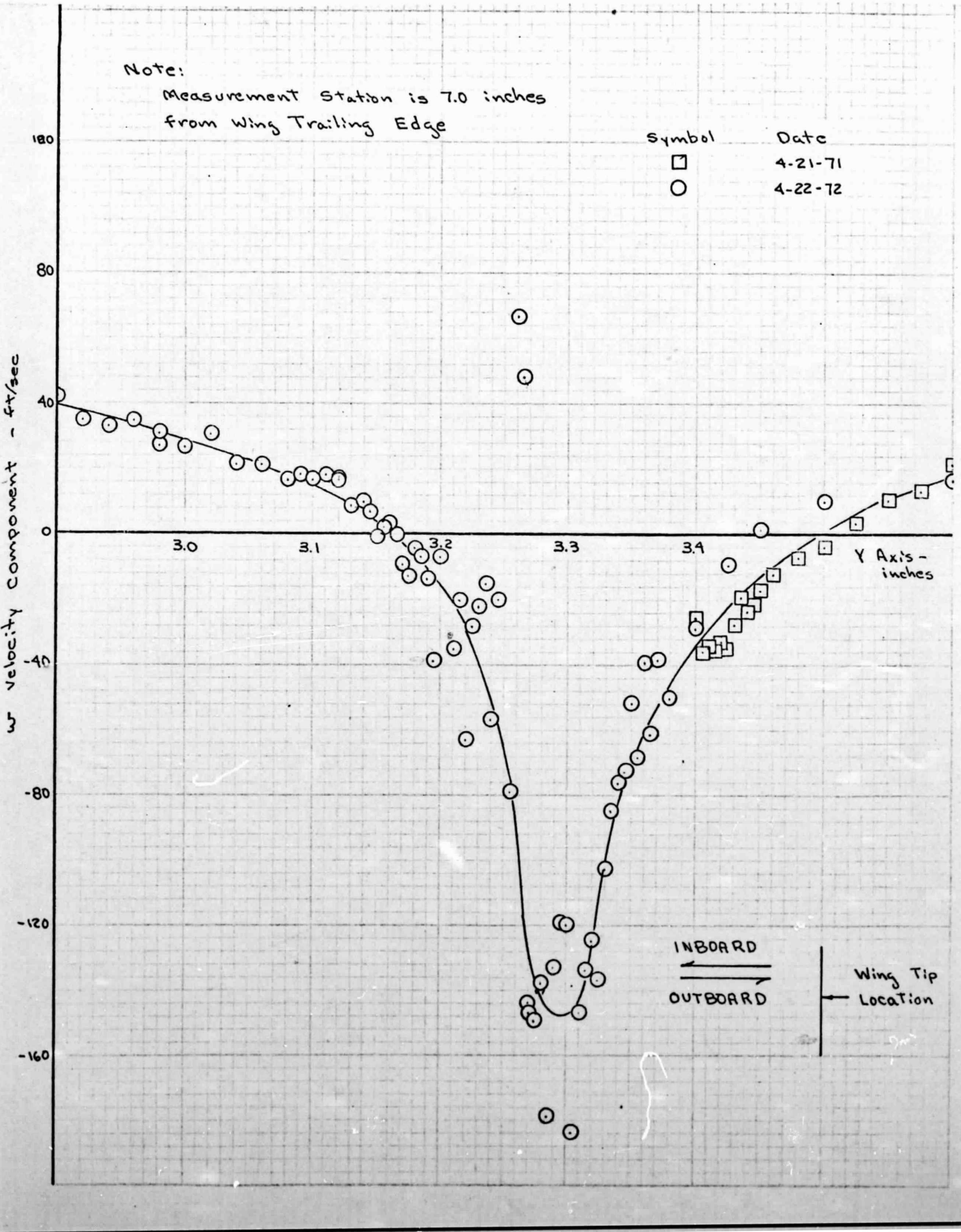

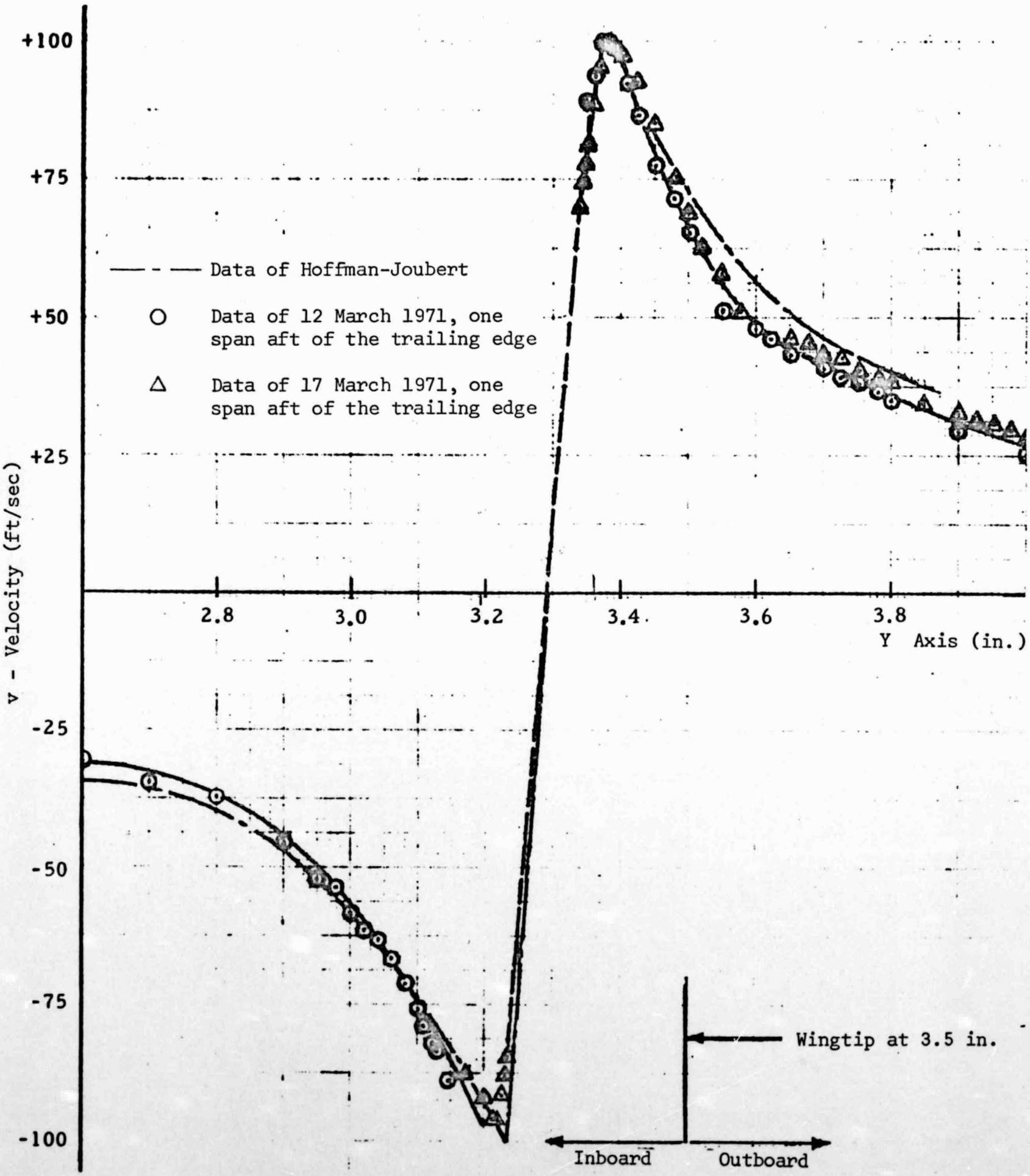

Figure 23 Comparison of v Velocity Component with Hoffman-Joubert Tangential Velocity Predictions